Catalysis Science & Technology

Accepted Manuscript

ROYAL SOCIETY OF CHEMISTRY

www.rsc.org/catalysis

Catalysis Science & Technology RSCPublishing

MINIREVIEW

Hydrogen Energy Future with Formic Acid: A Renewable Chemical Hydrogen Storage System

Cite this: DOI: 10.1039/x0xx00000x

Received 00th August 2015,
Accepted 00th August 2015

DOI: 10.1039/x0xx00000x

www.rsc.org/

Ashish Kumar Singh*[,a], Suryabhan Singh*[,b] and Abhinav Kumar*[,c]

Formic acid, the simplest carboxylic acid, is found in nature or can be easily synthesized in laboratory (major by-product of some second generation biorefinery processes), an important chemical due to its myriad applications in pharmaceuticals and industries. In recent year, formic acid has been used as an important fuel either without reformation (in direct formic acid fuel cells, DFAFCs) or with reformation (as potential chemical hydrogen storage material). Owing to the better efficiency of DFAFCs compared to several other PEMFCs and reversible hydrogen storage, formic acid could serve as one of the better fuel for portable devices, vehicles and other energy related applications in future. This review is focused on the recent developments of formic acid as reversible source for hydrogen storage. Recent developments in this direction will likely give access to a variety of low-cost and highly efficient rechargeable hydrogen fuel cells within the next few years by use of suitable homogeneous metal complex/heterogeneous metal nanoparticle based catalysts under ambient reaction conditions. The production of formic acid from atmospheric CO_2 (a green-house gas) will decrease the CO_2 content and may be helpful in reducing the global warming.

1. Introduction

It is well known that the non-renewable fossil fuels can sustain only for next few decades. In future, there will be the strong demand for safe and renewable energy carrier for transportation and other energy related applications. Several people are actively working in different fields such as solar energy conversion, lithium ion batteries, geothermal power and nuclear energy, which could cope up the energy problem for long time. Hydrogen is a promising and widely considered option as an alternative energy feedstock, despite extensive efforts by the researchers to use hydrogen as a possible energy source, its storage and transportation is a major hurdle to use it directly.[1-12] To use hydrogen as a clean fuel and to overcome the hurdles in its safe and efficient storage, various advanced research approaches for the development of new materials, that can store and deliver hydrogen at acceptable rates, have been discovered.[1-12] Based on the methods, it can be mainly divided in two ways either physical or chemical storage.[1-13]

In physical storage method, hydrogen is stored in its diatomic molecular form either in closed container at high pressure and low temperatures such as using high-pressure tanks or cryo-compression[14,15] or getting it adsorbed on high surface area materials *viz.* various carbon materials,[16-19] zeolites,[20,21] clathrate hydrates,[22,23] or recently the most developed or attractive material metal-organic frameworks.[12,24-27] However, hydrogenation/dehydrogenation energy levels of these materials have a large energy gap, hence, are usually less energy efficient. In chemical storage method, hydrogen is stored in the chemically bonded form instead of its molecular form. Usually, some suitable molecules having higher hydrogen content have been selected which could release hydrogen efficiently under ambient conditions either via a catalytic or non-catalytic process. For example, sodium borohydride, ammonia borane, formic acid, hydrous hydrazine, metal hydrides, metal borohydrides, metal amidoborates, etc.[2-10] Among them, formic acid is widely explored as possible fuel for fuel cells because of the properties such as non-toxic (although neat formic acid is corrosive and its vapour is harmful), liquid at room temperature, high density (1.22 g cm^{-3}) and normal handling conditions (8.4-100.8 ºC).[2-11]

Formic acid is most commonly found in nature in the bites and stings of insects[28] and is major by-product of petroleum refining (naphtha partial oxidation; methanol carbonylation/methyl formate hydrolysis), biomass processing, and several industrial organic syntheses. Hydrogen is easy to produce from electrolysis of water.[29] Scientists have been able to produce formic acid by hydrogenation of CO_2 present in the

atmosphere or separated from in industrial waste[30] using suitable catalysts.[31-34]

Dr. Ashish Kumar Singh was born in Varanasi, U. P., India in 1985. He received his Ph.D. degree in Inorganic Chemistry from Banaras Hindu University, Varanasi, India in 2011. He then worked with Prof. Qiang Xu, AIST as a JSPS postdoctoral fellow between 2011-2013. He is currently working as DSK postdoctoral fellow in the group of Prof. B. R. Jagirdar at IPC, IISc. He is currently interested in the development of homo-/heterogeneous catalysts for the activation of small molecules for chemical hydrogen storage.

Dr. Suryabhan Singh was born in Varanasi, U. P., India in 1982. He received his M.Sc. in Chemistry in 2007 and Ph.D. degree in Inorganic Chemistry under the supervision of Prof. S. Bhattacharya from Banaras Hindu University, Varanasi, India in 2013. He is currently working as DSK postdoctoral fellow in the group of Prof. S. Natrajan at SSCU, IISc. His research work is focused on the development of metal organic frameworks for catalytic and gas storage applications.

Dr. Abhinav Kumar was born in Varanasi, U. P., India in 1979. He received his Ph.D. degree in Inorganic Chemistry under the supervision of Prof. N. Singh, from Banaras Hindu University, Varanasi, India in 2009. He is working as Assistant Professor at Department of Chemistry, University of Lucknow, India since 2009. His research work is focused on the development of organometallic/coordination compounds for photovoltaic and material applications.

Formic acid (FA) is considered as one of the most promising materials for hydrogen storage today. Despite the hydrogen content (4.4 wt%) in FA is less than the target set by the US Department of Energy for 2012[35] it surpasses that of the most other *state-of-the-art* storage materials utilized today owing to its simplicity and useable/net capacity.[3] Useable or net capacity is defined as the effective hydrogen content that can be recovered in the form of H_2 from the Chemical Hydrogen storage system.[36] The produced H_2 can be utilized for clean electricity production at low-temperature with the production of merely H_2O. In fact, gravimetric energy density of formic acid is 7 times superior compared to commercial lithium ion batteries.[37,38] Besides the formic acid, hydrogen generation from other liquid organic molecules, also named as liquid-organic hydrogen carriers (LOHC)[39,40] has been extensively studied e.g. methanol,[41,42] carbazole, cycloalkanes etc. However, these systems have diverse problems for use as hydrogen storage materials, such as toxicity, cost, limited stability, low dehydrogenation kinetics, and low efficiency of the regeneration processes.

Formic acid has also been considered as a fuel in direct formic acid fuel cells (DFAFCs).[43] Chemical processes in DFAFCs involves two electron direct oxidation of formic acid at the anode and two electron reduction of O_2 at the cathode (Eqs. (1-3). However, in addition to the fuel crossover and catalyst deactivation, DFAFCs suffer from more specific detrimental effects: CO from the dehydration of FA through undesired route (Eq. 4) poisons the catalysts (already 20 ppm destroy the fuel cell).

Anode:

$$HCOOH \rightarrow CO_2 + 2H^+ + 2e^- \qquad E^0 \sim -0.25\ V \qquad (1)$$

Cathode:

$$1/2O_2 + 2H^+ + 2e^- \rightarrow H_2O \qquad E^0 = 1.23\ V \qquad (2)$$

Overall:

$$HCOOH + 1/2O_2 \rightarrow CO_2 + H_2O \qquad E^0_{Cell} \sim 1.48\ V \qquad (3)$$

Undesired route

$$HCOOH \rightarrow -CO_{ads} + H_2O \qquad (4)$$

Sometimes the catalyst's active phase is prone to FA corrosion and the FA's hydrophilicity can dehydrate the proton exchange membrane (PEM) and cause increased cell resistance.

In recent years, immense progress has been made and many examples have been reported on efficient use of formic acid as renewable source of energy with the great efforts of researcher all over the world.[1-10] This review provides an overview of catalytic hydrogen release and regeneration/production of formic acid. First part is focused on decomposition of formic acid for chemical hydrogen storage using suitable homo-/heterogeneous catalyst. Second part is particularly dealing with the production and regeneration of formic acid from various processes such as biomass conversion, hydrogenation of CO_2 and third part gives an overview for the recent developments in the practical set up for formic acid based "Rechargeable Hydrogen Batteries". In the last section, we will briefly discuss the current research progress, expected improvements and future outlook in this research area.

2. Formic acid decomposition

The challenge of producing, storing and transporting hydrogen affordably has kept fuel cells from becoming popular. Instead of transporting hydrogen gas, it is more practical to have a hydrogen-containing material or chemical hydrogen storage material that can be broken down under ambient conditions to generate H_2 gas whenever required.

Formic acid, containing 4.4 wt.% hydrogen, can be decomposed following two principal pathways (Eq. (1) and

(2)), in which the process producing CO_2 and H_2 (5) is the desired reaction and that producing CO and H_2O (6) is the undesired side reaction.[3-10]

$$HCOOH \rightarrow H_2 + CO_2 \qquad \Delta G = -32.9 \text{ kJ mol}^{-1} \qquad (5)$$

$$HCOOH \rightarrow H_2O + CO \qquad \Delta G = -28.5 \text{ kJ mol}^{-1} \qquad (6)$$

CO-free decomposition of formic acid through pathway 1 is crucial for the formic acid based hydrogen storage.[3-10] The combination of carbon dioxide and formic acid as hydrogen storage system might act as an elegant and simple concept wherein selective decomposition of formic acid to H_2 and CO_2 and recycling of CO_2 by reduction in the presence of H_2 to formic acid can be achieved. Meanwhile, the abundance of CO_2 on the earth makes it cheap and readily available chemical. In this case, decreasing CO_2 emissions by reduction using H_2 makes CO_2 itself as a hydrogen carrier. Tremendous research have been done in search of the suitable catalysts (homo-/heterogeneous) for selective decomposition of FA. However, to achieve the complete selectivity for decomposition of formic acid through desired pathway is still a challenging task.

2.1 Homogeneous catalysts

Over the last few years, there has been remarkable increase in the research activities in search of high-performance homogeneous catalysts for hydrogen release from formic acid. Various groups have highlighted performances of these homogeneous catalysts in excellent review articles.[3-10] Pioneering study by Coffey in 1967,[44] described the use of soluble Pt, Ru and Ir phosphine complexes for selective decomposition of formic acid to H_2 and CO_2. Among all the complexes, iridium complex $IrH_2Cl(PPh_3)_3$ gave the highest rate of decomposition. $Rh(C_6H_4PPh_2)(PPh_3)_2$, an organometallic complex, is active for the decomposition of formic acid.[45] Platinum dihydride complex catalyzed the reversible formation of carbon dioxide and hydrogen from formic acid. The process was somewhat dependent on the choice of solvent and promoted by the addition of a small amount of sodium formate.[46] King and Bhattacharyya observed that nitrate ions were promoting the formic acid decomposition reaction catalyzed by rhodium(III) catalyst.[47] Reactivity of a hydride and equivalent halide complexes of molybdenum were studied for formic acid decomposition. It is observed that the use of the hydride is important for catalysis, as the equivalent halide complexes were inactive.[48] Puddephatt and co-workers have studied the detailed mechanism of formic acid decomposition process over a binuclear, diphosphine-bridged, diruthenium catalyst $[Ru_2(\mu\text{-CO})(CO)_4(\mu\text{-dppm})_2]$ and characterized the intermediates of FA decomposition process using X-ray crystallography.[49,50] This complex catalyzes the reversible formation/decomposition of FA.

2.1.1 Noble-Metal Catalysts

Systematic studies for hydrogen generation by catalytic decomposition of formic acid have been performed by the groups of Beller and Laurenczy.[51-53] Majority of catalysts active for the selective dehydrogenation of formic acid are complexes of ruthenium and iridium. However, recently some catalyst systems, based on non-noble metals such as Fe and Al, have also been reported. Beller and co-workers investigated the decomposition of formic acid with different homogeneous catalysts at 313 K, including metal salts $RhCl_3{\cdot}xH_2O$, $RuBr_3{\cdot}xH_2O$ and precursors $[\{RuCl_2(p\text{-cymene})\}_2]$, $[RuCl_2(PPh_3)_3]$, $[\{RuCl_2(\text{benzene})_2\}_2]$ etc, in the presence of amine/phosphine/salts as adducts.[51-53] The activity of these catalysts depend upon type of adducts and their concentration. High catalytic activity for the decomposition of formic acid/amine adducts of different compositions were achieved by variety of Ru precursors and phosphine ligands.[52] With $RuBr_3{\cdot}xH_2O/PPh_3$ catalyst system (with 3.4 equiv. PPh_3, TOF 3630 h^{-1} after 20 min) the best activity was observed for hydrogen generation using 5 HCO_2H/2 NEt_3 adduct. They have checked the activity for the dehydrogenation of FA in the presence of $[\{RuCl_2(p\text{-cymene})\}_2]$ and 22 amidines adducts.[53] The activity of the catalyst systems were depending on the nature of the bases and their ratio to formic acid. For majority of bases, an increase in concentration improved the catalyst activity. In general, in the presence of tertiary alkyl amines or more basic amidines, higher activities for FA dehydrogenation were achieved. Further, investigation for the effect of different additives revealed that the presence of halide ions was also influencing the rate of hydrogen generation significantly. Best result with $[RuCl_2(p\text{-cymene})]_2$ as pre-catalyst was obtained by addition of 10 equiv of KI. This catalyst system has activity >450% better than $[RuCl_2(p\text{-cymene})]_2$. They also observed that amine adducts have no significant effect on hydrogen production by $[RuCl_2(\text{benzene})]_2/PPh_3$ catalyst system while with triethylamine (NEt_3) (3:4; amine to HCO_2H) or *N,N*-dimethyl-*n*-hexylamine (4:5), fast hydrogen generation observed with $[RuCl_2(\text{benzene})]_2$/dppe (TON = 1644 and 1469 h^{-1}, respectively).

A series of amine-functionalized ionic liquids (ILs) prepared and used for hydrogen generation by the selective catalytic decomposition of formic acid in the presence of $[\{RuCl_2(\text{p-cymene})\}_2]$ catalyst.[54,55] Amongst the investigated ILs, the 1-(2-diisopropylaminoethyl)-3-methylimidazolium chloride–sodium formate ($iPr_2NEMimCl$–HCOONa) system exhibited high activity (TOF > 600 h^{-1}) at 333 K. However, this process was not recyclable. Wasserscheid and co-workers reported an outstandingly simple, active and recyclable ionic liquid-based system for the catalytic decomposition of formic acid. The most efficient catalytic system is $RuCl_3$ dissolved in 1-ethyl-2,3-dimethylimidazolium acetate. This catalyst system converted formic acid to hydrogen and carbon dioxide selectively and was recyclable for at least nine cycles without deactivation or change in selectivity.[56] Decisively; this simple catalytic system exhibits TOFs of 150 h^{-1} at 353 K and 850 h^{-1} at 393 K.

Laurenczy and co-workers carried out decomposition of FA/sodium formate solution using hydrophilic ruthenium-based catalysts, generated from the highly water-soluble ligand *meta*-

trisulfonated triphenylphosphine (TPPTS) with either $[Ru(H_2O)_6]^{2+}$ or, more conveniently, commercially available $RuCl_3$.[57,58] This catalyst system could operate over a wide range of pressure, under mild conditions, and at a controllable rate without CO contamination. Later, they immobilized this catalyst on various supports using ion exchange, coordination or physical absorption methods, to get advantage of recycling, especially for dilute formic acid solutions, or for mobile, portable applications of heterogenized catalysts.[59]

Wills and co-workers investigated activity of FA dehydrogenation by several Ru^{II} and Ru^{III} catalyst precursors ($[Ru_2Cl_2(DMSO)_4]$, $[RuCl_2(NH_3)_6]$, $RuCl_3$ and $[Ru_2(HCO_2)_2(CO)_4]$) in triethylamine at 393 K, explicitly without adding phosphine ligands.[60] As can be expected for such high temperatures, FA decomposition activities are exceptionally high (up to *ca.* 1.8×10^4 h^{-1}). Unfortunately, the CO concentration consistently exceeded 200 ppm for all the catalysts tested. The authors suggested the formation of $[Ru_2(HCO_2)_2(CO)_4]$ as the active species common to all the precursors under these reaction conditions. It is interesting to note that during reuse, all the catalysts exhibited a slight enhancement in activity with each run, indicating ongoing formation of the active catalyst species. Later, same group used their $[Ru_2Cl_2(DMSO)_4]/NEt_3$ system in an attempt to continuously decompose formic acid at a rate approaching the catalyst's maximum activity without acid accumulation in the system.[61] Of the two concepts tested–one temperature based and the other using an impedance probe–the latter gave promising results, even though the gas flow decreased slightly over several days.

Homogeneous Ru catalysts based on polydentate tripodal ligands 1,1,1-*tris*-(diphenylphosphinomethyl)ethane (triphos) and *tris*-[2-(diphenylphosphino)ethyl]amine (NP_3), which can either be prepared *in situ* from suitable Ru(III) precursors or as molecular complexes, exhibited moderate to good activity for the selective formic acid dehydrogenation to CO_2 and H_2.[62] The complex $[Ru(\kappa^3\text{-triphos})(MeCN)_3](OTf)_2$ showed superior performances with a TON of 10000 after 6 h using 0.01 mol% of the catalyst and allowed recycling up to eight times (0.1 mol% catalyst) with a total TON of 8000 after *ca.* 14 h of continuous reaction at 353 K in the presence of *n*-octyldimethylamine ($OctNMe_2$). Preliminary mechanistic NMR studies using *in situ* generated $[Ru(\kappa^3\text{-triphos})(MeCN)_3](PF_6)_2$ and molecular complex $[Ru(\kappa^4\text{-}NP_3)Cl_2]$ demonstrated that the NP_3 ligand helps to stabilise Ru-hydrido species, hence there is subtle differences in activity due to the ligand effects. Later to clarify the mechanism of catalytic dehydrogenation of formic acid (whether a metal-centered inner-sphere or a ligand-centered outer-sphere pathway) by the aforementioned complexes, an integrated experiment-theoretical study have been performed (Fig. 1).[63] Mechanism is depending on the choice of polydentate phosphines, i.e., triphos *vs.* NP_3 and the nature and number of ancillary ligands (Cl *vs.* MeCN), making available a different number of vacant coordination sites for activation of catalysts to their active forms. From the mechanistic study, it was concluded that Ru-hydrido *vs.* Ru-formato species are pivotal to bring about the efficient release of H_2 and CO_2 following either a metal-centered (inner-sphere) or a ligand-centered (outer-sphere) pathway, respectively.

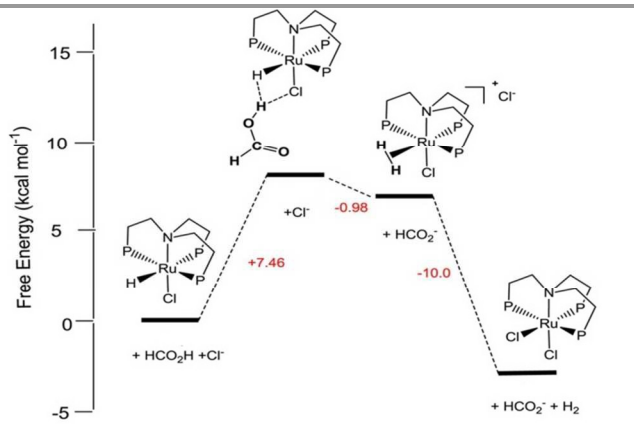

Fig. 1 Schematic reaction pathway for formic acid dehydrogenation by $[Ru(\kappa^4\text{-}NP_3)Cl_2]$. Reprinted with permission from ref. 63. Copyright 2013 American Chemical Society

Enthaler *et al.* performed a preliminary study on the ruthenium-catalysed decomposition of formic acid to yield hydrogen by applying a ruthenium complex modified polyformamidine network as a solid catalyst.[64] The polyformamidine acted as a dual support for $[RuCl_2(p\text{-cymene})]_2$ or $[RuCl_2(p\text{-cymene})]_2/PPh_3$: on the one hand as a ligand and on the other hand as a base for the activation of formic acid. It is noteworthy that polyformamidine supported $[RuCl_2(p\text{-cymene})]_2/PPh_3$ catalyst system has a higher activity (TON = 325 for 3h) than the unsupported $[RuCl_2(p\text{-cymene})]_2/PPh_3$ with NEt_3 addition (TON = 169 for 3h).

Fukuzumi *et al.* reported FA dehydrogenation, catalyzed by a water-soluble Rh catalyst, $[Rh^{III}(Cp^*)(bpy)(H_2O)](SO_4)$ (Cp^* = pentamethylcyclopentadienyl, bpy = 2,2′-bipyridine) in aqueous solution at room temperature.[65] Similarly, an iridium catalyst $[Ir^{III}(Cp^*)(dhbpy)(H_2O)](SO_4)$ (dhbpy = 4,4′-dihydroxy-2,2′-bipyridine) was reported by Himeda for CO-free FA dehydrogenation.[66] High catalytic activity (TOF = 14000 h^{-1} at 363 K) without deterioration of the catalyst in the continuous runs were observed for this catalytic system. They also demonstrated that heteronuclear iridium–ruthenium complexes $[Ir^{III}(Cp^*)(H_2O)(bpm)Ru^{II}(bpy)_2](SO_4)_2$ {bpm = 2,2′-bipyrimidine} is highly active catalyst for hydrogen generation in an aqueous solution under ambient conditions giving a TOF of about 426 h^{-1}.[67]

In 2013, a new bisMETAMORPhos (MMP) ligand and its iridium complexes (Ir-MMP), in which the ligand is in the dianionic state, are reported by Reek and co-workers (Scheme 1).[68] The anionic form of the ligand MMP functions as an internal base, hence this catalyst system is active for FA dehydrogenation in "base-free" conditions. Base-free dehydro genation of formic acid is important as it can act as a convenient carrier for hydrogen storage, because it increases the hydrogen content from 2.3 wt % in typical $HCOOH/NEt_3$

5:2 mixtures to 4.4 wt % in pure HCOOH. Ir-MMP catalyst is not only operates under such base-free conditions, but also produces clean, CO-free dihydrogen and is very robust and active (base free, TOF 3092 h^{-1} in toluene). As such, the coope-

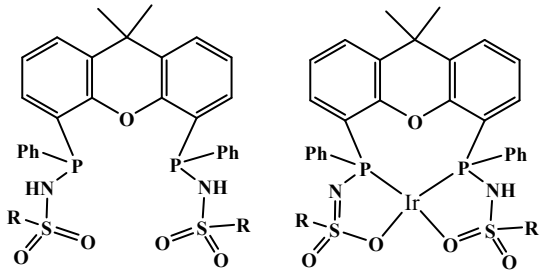

Scheme 1 Structure of bisMETAMORPhos (MMP) ligand and its Ir complex (Ir-MMP). (Where R = 4-t-butylphenyl).

-rative catalysis concept, employing a bifunctional ligand, may hold promise for the efficient and effective (storage and) release of H_2 ideally generated from a renewable source, such as solar energy.

2.1.2 Non-noble metal catalysts. First non-noble metal-based homogeneous catalyst system for hydrogen generation from formic acid, was reported by Beller, Ludwig and co-workers. Boddien *et al.* reported FA dehydrogenation by a catalyst formed *in situ* from inexpensive $Fe_3(CO)_{12}$, 2,2′:6′2″-terpyridine or 1,10-phenanthroline, and triphenylphosphine, under visible light irradiation at room temperature.[69] Depending on the kind of *N*-ligands significant catalyst turnover numbers (>100) and turnover frequencies (up to 200 h^{-1}) were observed. Experimental (NMR, IR studies), and theoretical (DFT) studies of iron complexes, which are formed *in situ* under reaction conditions, confirmed that PPh_3 plays an active role in the catalytic cycle and that *N*-ligands enhances the stability of the system. It is shown that the reaction mechanism includes iron hydride species which are generated exclusively under irradiation with visible light.[69]

Later, they demonstrated another *in situ* generated iron based system as a highly active catalyst (TON up to 100000 and TOF nearly 10000 h^{-1}) for the CO-free decomposition of formic acid in a common organic solvent (propylene carbonate) without any further additives or light (Fig. 2, Table 1).[70] The catalyst can be formed *in situ* from $Fe(BF_4)_2 \cdot 6H_2O$ and a tetradentate phosphine ligand *tris*[(2-diphenylphosphino)ethyl] phosphine (PP_3) under the reaction conditions or can be added to the reaction mixture in a pre-synthesized form as

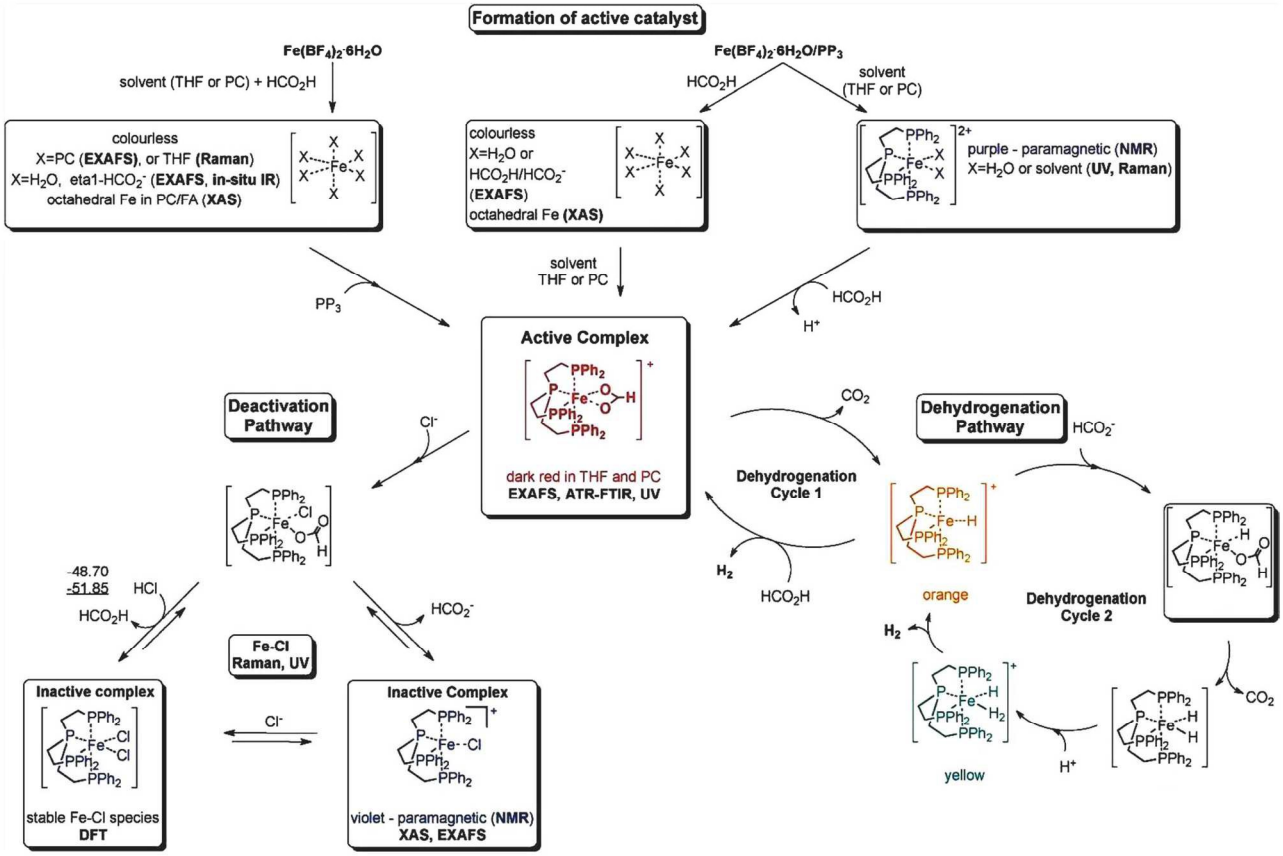

Fig. 2. Summary of the activation and deactivation pathways of the $Fe(BF_4)_2 \cdot 6H_2O/PP_3$ catalyst system as well as proposed species formed based on the results of spectroscopic analyses. Free enthalpies calculated at the B3PW91/6-31G (including polarization functions except those of hydrogen) and B3PW/6-311G (including polarization functions also for hydrogen; value underlined) levels of theory. The relative enthalpies of the reaction of the interconversion are given in kJ mol^{-1}. It is assumed that iron retains the formal oxidation state +II. Reprinted with permission from ref. 71. Copyright 2014 Wiley-VCH.

$[FeH(PP_3)]^+$. During the process, iron cation is permanently coordinated to four phosphorus centers of PP_3 while the remaining two coordination sites are occupied by the HCOOH substrate and/or product-derived species during the catalytic cycle. Spectroscopic studies and density functional theory calculations suggested two possible pathways for H_2 release from HCOOH, both of which went through a common Fe-hydride species, $[FeH(PP_3)]^+$.[70]

Table 1. Selective dehydrogenation of FA in the presence of in situ generated iron/non-noble catalysts.[a] (Adopted with permission from ref. 71)

Metal precursor	*T* (K)	V_{2h} (mL) V_{3h} (mL)	TON_{2h} TON_{3h}	Yield (%)	CO (ppm)	Refs
$Fe(BF_4)_2{\cdot}6H_2O$	313	333 505	1279 1942	100	<1	70
$[Fe(acac)_2]$	313	315 486	1217 1879	100	<1	71
$[Fe(acac)_3]$	313	324 503	1253 1943	100	<1	71
$Fe(ClO_4)_2{\cdot}xH_2O$	313	258 388	997 1500	100	<1	71
$Fe(ClO_4)_3{\cdot}xH_2O$	313	240 367	928 1418	100	<1	71
$Fe(OAc)_2$	313	245 489	945 1889	98	70	71
$[Fe_3(CO)_{12}]$	333	84 131	325 505	–	1120	71
$[Fe(CO)_3COT]$	333	7.8 33	30 128	–	450	71
$FeCl_2$[b]	333	0.4 0.8	1.4 3.0	–	<10	71
$FeCl_3$[c]	333	0 0	– –	–	<10	71
$Co(BF_4)_2{\cdot}6H_2O$	333	27 51	103 197	–	<10	71
$[Mn(acac)_2]$[b]	333	0.15 0.23	0.6 0.9	–	<10	71
$Fe(BF_4)_2{\cdot}6H_2O$	333	1583 2101	6119 8117	89	<1	71

[a] Reaction conditions: 5.3 µmol metal precursor (100 ppm) plus 10.6 µmol PP_3 (**1**) were added to 2 mL FA and 5 mL PC at 313 or 333 K. The volume of gas was measured with an automatic gas burette and analyzed by GC (H_2/CO_2, 1:1). [b] Traces of H_2 detected. [c] No H_2 detected. All values given are corrected by the value of a blank reaction without catalyst as reference. Values are an average of at least two experiments and have an error within 10 %

Recently, they have extensively studied the iron-catalyzed dehydrogenation of formic acid both experimentally as well as mechanistically.[71] The active catalysts were generated *in situ* from different cationic Fe^{II}/Fe^{III} precursors and PP_3 (Table 1). These catalysts are active at amine-free and ambient conditions, and the activity of these catalysts were highly dependent on the nature of solvent used, the presence of halide ions, the water content, and the ligand-to-metal ratio. The optimal catalytic performance was achieved by using $[FeH(PP_3)]BF_4/PP_3$ in propylene carbonate in the presence of traces of water. With the exception of fluoride, the presence of halide ions in solution inhibited the catalytic activity. The *in situ* transmission FTIR measurements revealed the formation of an active iron formate species (evidenced by the band observed at 1543 cm^{-1}), which could be correlated with the evolution of gas. This active species was deactivated in the presence of chloride ions due to the formation of a chloro species.

Milstein and co-workers reported iron based PNP pincer complex [(^{t}Bu-PNP)Fe(H)$_2$(CO)] (^{t}Bu-PNP = 2,6-bis(di-tert-butylphosphinomethyl)pyridine) as an efficient and selective catalyst for the decomposition of formic acid to carbon dioxide and hydrogen at 313 K in the presence of trialkylamines with turnover numbers of up to 100,000.[72] From experimental studies, it is observed that catalytic process proceeds *via* protonation of the iron dihydride catalyst, followed by dihydrogen liberation which led to an unsaturated species that is transformed into a hydrido–formate complex. Regeneration of the iron dihydride catalyst is finally achieved by CO_2 elimination. This step is predicted to proceed through a novel, non-classical intramolecular β-H elimination according to DFT calculations.

In another recent work, Bielinski *et al.* reported a homogeneous iron catalyst that gives approximately 1,000,000 turnovers for FA dehydrogenation, when used with a Lewis acid co-catalyst.[73] To date, this is the highest turnover number reported for a first-row transition metal catalyst. Based on the preliminary studies, they suggested that the Lewis acid assisted in the decarboxylation of a key iron formate intermediate as shown in Scheme 2. They have studied promotion of catalysis by different Lewis acids and observed that the highest TON and TOF were achieved with alkali or alkaline earth metal salt co-catalysts. Importantly, the enhancement of activity is associated with the chemical affinity for carboxylate. Best results obtained for $LiBF_4$ containing an alkali metal ion (Li^+) and a weakly coordinating ligand (BF_4^-).

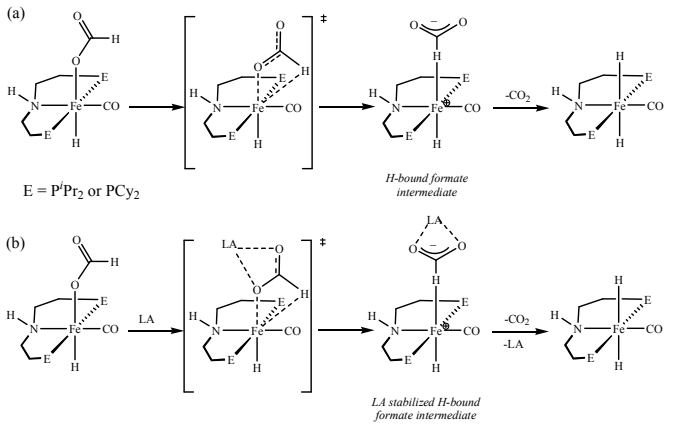

Scheme 2. Proposed pathway for decarboxylation of Fe catalysts in the absence (a) and presence (b) of a lewis acid. Adopted with permission from ref. 73. Copyright 2014 American Chemical Society

Complete FA dehydrogenation was obtained using 0.01 mol% catalyst 10 mol% Lewis acid (NaCl, $NaBF_4$, or $LiBF_4$). Among them, $LiBF_4$ was giving the fastest time for completion of reaction. In fact, with catalyst loadings as low as 0.0001 mol%, a TON of 983,642 and TOF of 196,728 h^{-1} were obtained. From this study, they concluded that this Lewis acid promotion was general for other catalysts used for FA dehydrogenation, as well as the reverse process i.e. CO_2 hydrogenation.

Myers and Berben reported first molecular aluminium complexes of the *bis*(imino)pyridine ligand, (PhI_2P^{2-})Al(THF)X where X = H or CH_3) for selective dehydrogenation of formic acid to H_2 and CO_2 with an initial

turnover frequency of 5200 turnovers per hour.[74] Low-temperature reactions show that reaction of Al-hydride complex with HCOOH afforded a complex that was protonated three times: twice on the PhI_2P^{2-} ligand and once to liberate H_2 or CH_4 from the Al-hydride or Al-methyl, respectively. In the absence of protons, insertion of CO_2 into the Al-hydride bond is facile and produces an Al-formate. Upon addition of protons, liberation of CO_2 from the Al-formate complex affords an Al-hydride. Deuterium labelling studies and the solvent dependence of the reaction indicated that outer sphere β-hydride abstraction supported by metal–ligand cooperative hydrogen bonding is the likely mechanism for C–H bond cleavage.

Based on the previous reports, a most commonly observed mechanism (It may not be applicable for all the catalyst system) for catalytic decomposition of formic acid by homogeneous catalysts could be given as Scheme 3. These reactions have following steps: (1) Deprotonation of formic acid to formate either itself or by addition of base, (2) formation of metal formate complex, (3) the most important and rate determining step is β-hydride elimination of CO_2 and finally (4) elimination of CO_2 and H_2.

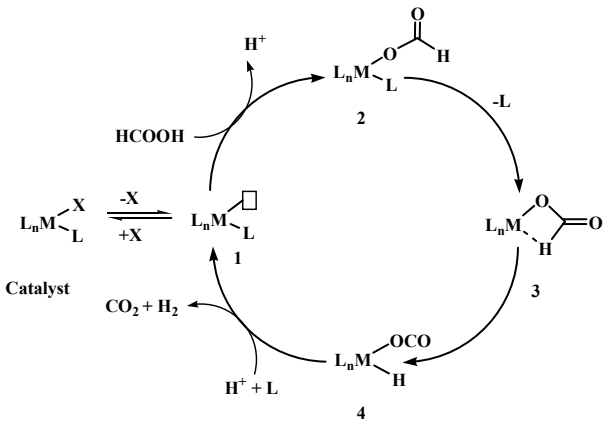

Scheme 3. A general mechanism for catalytic decomposition of formic acid.

As the β-hydride elimination is rate determining step, the catalyst having tendency to stabilize structure 3 have better activity for formic acid dehydrogenation. This goal could be achieved not only by modifying metal centre/geometry of metal centre/ligands geometry of homogeneous catalysts but by using different kind of bases as well as other additive e.g. lewis acids, solvents (ionic liquids) etc. In some cases, base-free dehydrogenation achieved because of the presence of basic sites in catalysts itself or basic ionic liquid. Further, search for suitable reaction condition and homogeneous catalyst based on non-noble metals for selective dehydrogenation of formic acid are still under progress.

2.2 Heterogeneous catalysts

Initially, decomposition of formic acid using heterogeneous catalysts have been mainly performed in gas phase[10] using the metal,[75-78] metal oxides[79-84] and metal supported on oxides or carbon catalysts.[85-93] A gas phase reaction required introduction of an inert carrier gas to dilute formic acid below its saturated vapor pressure or heating above the normal boiling point of formic acid (>373 K). However, researchers had also studied hydrogen generation from formic acid decomposition in liquid-phase or at low temperature. Table 2 summarizes selected heterogeneous catalysts for the decomposition of aqueous formic acid to hydrogen and carbon dioxide. Most of the heterogeneous catalysts are supported mono-/bi-/trimetallic nanoparticles with Pd as a major component.

Xing and co-workers found that Pd-Au/C and Pd-Au@Au/C have a unique characteristic of evolving high-quality hydrogen from the catalytic decomposition of liquid formic acid in the presence of sodium formate (HCOONa) as a base at convenient temperature.[94,95] Order of catalytic activity based on TOF values is Pd/C < Pd-Cu/C < Pd-Ag/C < Pd-Au/C. Higher catalytic activities of bimetallic Pd-Ag/C and Pd-Au/C catalysts were attributed to the higher tolerance of Ag and Au with respect to CO poisoning. Catalytic activity was further improved by the addition of $CeO_2(H_2O)_x$ because the CeO_2 produces cationic palladium species, which showed high activity in CO oxidation[96] and methanol decomposition.[97] Another reason was that $CeO_2(H_2O)_x$ on the Pd surface can induce the decomposition of formic acid by a more efficient route, in which fewer poisoning intermediates would be produced.[94]

Later, they reported a novel Pd-Au bimetallic catalyst with a Pd-Au@Au core-shell nanostructure supported on carbon. This was synthesized by a simultaneous reduction method without using any stabilizer and was successfully used as the catalyst for hydrogen generation by formic acid decomposition. The catalyst exhibited high activity, selectivity and stability at a low temperature and the catalytic performance was much better than that for the corresponding monometallic catalysts. Especially, the reforming gas from formic acid decomposition contained only 30 ppm of CO and can be used directly to feed the fuel cells.[95] Inspired by promotion effect of CeO_2 on catalytic activities of Pd-Au/C and Pd-Ag/C catalysts, they extended their investigations on other rare earth elements (Dy, Eu, and Ho) and obtained TOFs 269±202, 387±292, 224±73, and 45±11 h^{-1} for Pd-Au-Dy/C, Pd-Au-Eu/C, Pd-Au-Ho/C and Pd-Au/C catalysts, respectively, at 365 K.[98] In addition, these catalysts were active even at room temperature temporarily and above 325 K steadily. All the rare earth metal oxides-promoted catalytic activity of Pd-Au/C catalysts showed lower activation energies for decomposition of formic acid than Pd-Au/C and Pd-Au-Eu/C (84.2±7.4 kJ mol^{-1}). The metal/metal oxide catalysts composed of platinum, ruthenium and bismuth, denoted as $PtRuBiO_x$, are catalyze the selective dehydrogenation of FA in water at nearly ambient temperature.[99] The observed activation energy was 37.3 kJ mol^{-1} and TOF was estimated to be 312 h^{-1} in the first hour of the decomposition.

Table 2. Selected heterogeneous catalysts for the decomposition of aqueous formic acid.

Catalyst	TOF(h^{-1})	T (K)	Ref.
PdAu/C	27	365	94
PdAu/C-CeO_2	227	365	94
PdAu@Au	-	365	95
Pd-Au-Dy/C	269	365	98
Pd-Au-Eu/C	387	365	98
Pd-Au-Ho/C	224	365	98
$PtRuBiO_x$	312	353	99
Ag@Pd/C(core-shell)	125	293	100
	626	363	100
Pd/C	64	298	102
Au@Pd/N–mrGO	89.1	298	103
$Ag_{0.1}Pd_{0.9}$/rGO	105.2	298	104
$Co_{0.30}Au_{035}Pd_{0.35}$	80	298	105
$Ni_{0.40}Au_{0.15}Pd_{0.45}$/C	12.4	298	106
CoAuPd/DNA–rGO	85	298	107
Pd@SiO_2 or Pd/SiO_2	-	363	108
Pd@CN (N-doped carbon)	49.8	288	109
Pd/−$N(CH_3)_2$ Fc BR	820	348	110
Pd/MSC-30	2623	323	111
PdAu/MIL-101	-	363	112
AgPd($Ag_{80}Pd_{20}$)/MIL-101	848	353	113
Pd-NH_2-MIL-125	214	305	114
PdNi@Pd/GNs-CB	577	300	115
PdNi/GNs–CB	529	300	115
Au/Al_2O_3	-	353	89
Au@SiO_2	-	363	116
Au/ZrO_2	1590	323	117
1% Pt/C-NF	0.09 (s^{-1})	373	118
Pd-Ni-Ag/C	85	323	119
Pd/C	304	298	120
Pd-B/C	1184	298	120
Pd/mpg-C_3N_4	144	298	121

GN-graphene nanosheets, Fc BR = functionalized basic resin, CB-carbon black, N–mrGO = nitrogen-doped mildly reduced graphene oxide, CN-Nitrogen doped carbon, mpg-C_3N_4 = mesoporous graphitic carbon nitride

In an effort, Tsang and co-workers prepared various core-shell nanoparticles having an inner core of a metal element and an external shell of palladium.[100,101] Among all metals tested, the highest activity towards FA decomposition at room temperature is for Ag@Pd NPs (diameter 8 nm) with the thinnest continuous Pd shell (1-2 atomic layers) and corresponding Ag/Pd alloy and pure Pd catalysts showed very low activity.[100,101] Turnover frequencies per surface Pd site were comparable to homogeneous catalysts: 125 h^{-1} at 293 K and 252 h^{-1} at 323 K. At 293 K, an equimolar mixture of hydrogen and CO_2 was continuously produced without any trace of CO; on the other hand, CO was detected at temperatures higher than 323 K. Furthermore, theoretical calculations showed a strong correlation between the catalytic activity and the work function of the metal core: the largest net difference with the work function of the Pd shell led to the highest adsorption energy by charge transfer from the core to the shell, hence to the best possible activity of the resulting bimetallic structure for formic acid decomposition. The very short range of this so-called "ligand" electronic effect between the two metals explained why the highest performance was achieved for the thinnest Pd layer. Nanomaterials interface definitely plays a key role in catalysis.

Yan and co-workers have extensively studied catalytic dehydrogenation of formic acid using mono-/bi-/trimetallic nanoparticle based catalysts supported on different carbon materials.[102] Low cost Pd/C catalyst, synthesized *in situ* with citric acid, is reported for highly efficient CO-free hydrogen generation from formic acid/sodium formate aqueous solution at room temperature (Fig. 3).[102] Presence of citric acid during the formation and growth of the Pd nanoparticles on carbon drastically enhanced the catalytic property of the resulted Pd/C at room temperature (conversion efficiency 85% in 160 min and turnover frequency 64 mol H_2 mol^{-1} catalyst h^{-1}).

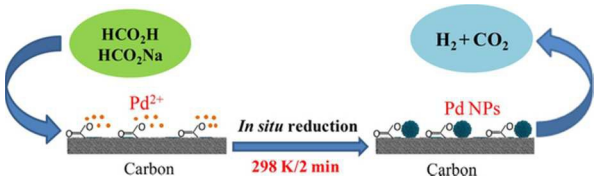

Fig. 3 Schematic presentation of Pd nanoparticle formation over carbon surface. Reprinted with permission from ref. 102. Copyright 2012 Nature Publishing group.

Ultrafine (1.8 nm) and well dispersed Au@Pd core–shell nanoclusters on nitrogen-doped mildly reduced graphene oxide (Au@Pd/N–mrGO), synthesized by a green and facile strategy, without any surfactant and additional reducing agent, exhibited much greater activity than its alloy or monometallic counterparts towards hydrogen generation from formic acid aqueous solution without using any additive at room temperature.[103] During the synthesis, N–mrGO acts as both reducing agent and support by taking advantage of its moderate reducing and high dispersing capabilties. In another report, they found that $Ag_{0.1}Pd_{0.9}$ nanoparticles assembled on reduced graphene oxide ($Ag_{0.1}Pd_{0.9}$/rGO) as an efficient catalyst for formic acid dehydrogenation reaction with 100% H_2 selectivity and exceedingly high activity at room temperature under ambient conditions.[104]

Yan and co-workers also reported $Co_{0.30}Au_{035}Pd_{0.35}$ nano-alloy supported on carbon as a stable, low-cost, and highly efficient catalyst for the CO-free hydrogen generation from formic acid dehydrogenation at room temperature.[105] The elevated stability of Co^0 in the protective nano-alloy structure makes its first application in FA dehydrogenation successful. More interestingly, the prepared Co-Au-Pd/C with the lower consumption of noble metals exhibits the 100% H_2 selectivity, highest activity, and excellent stability toward H_2 generation from FA without any additive at 298 K. The catalytic activities of $Co_{0.30}Au_{0.35}Pd_{0.35}$/C together with its mono-metallic (Pd/C, Au/C, and Co/C) and bi-metallic ($Au_{0.50}Pd_{0.50}$/C, $Co_{0.30}Pd_{0.70}$/C, and $Co_{0.30}Au_{0.70}$/C) counterparts for H_2 generation from FA decomposition at 298 K in ambient atmosphere are presented in Fig. 4. The as-prepared $Co_{0.30}Au_{0.35}Pd_{0.35}$/C exhibited a much better activity than those of mono- and bi-metallic catalysts synthesized by the same method. In a similar way, carbon supported highly homogeneous trimetallic NiAuPd alloy nanoparticles ($Ni_{0.40}Au_{0.15}Pd_{0.45}$/C) have also been employed as

catalyst for the selective dehydrogenation of formic acid.[106] This catalyst also exhibited high activity and 100% selectivity for dehydrogenation of FA without any additives at room temperature. The catalytic activity of $Ni_{0.40}Au_{0.15}Pd_{0.45}/C$ was much higher than its monometallic (Pd/C, Ni/C, Au/C) bimetallic counterparts ($Ni_{0.40}Pd_{0.60}/C$, $Au_{0.25}Pd_{0.75}/C$, $Ni_{0.40}Au_{0.60}/C$) as well as physical mixture of Ni/C, Au/C and Pd/C (Ni:Au:Pd = 0.40:0.15:0.45) under similar reaction conditions.

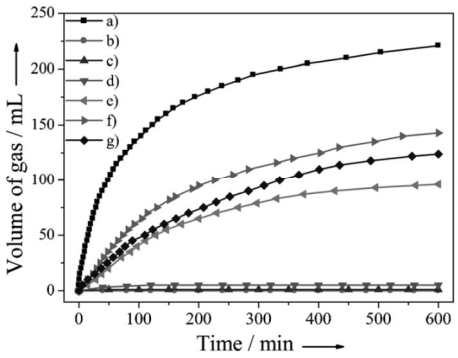

Fig. 4 Gas generation by decomposition of FA (0.5 M, 10 mL) versus time in the presence of a) $Co_{0.30}Au_{0.35}Pd_{0.35}/C$, b) Co/C, c) Au/C, d) $Co_{0.30}Au_{0.70}/C$, e) Pd/C, f) $Co_{0.30}Pd_{0.70}/C$ and g) $Au_{0.50}Pd_{0.50}/C$ (nmetal/nFA=0.02) at 298 K in ambient atmosphere. Reprinted with permission from ref. 105. Copyright 2013 Wiley-VCH.

They also reported DNA-directed and facile approach to synthesize the Co-Au-Pd/DNA–rGO composite (Co:Au:Pd = 1:1:1).[107] The catalytic performance of the Co-Au-Pd/DNA–rGO composite toward the dehydrogenation of FA without any additives at room temperature was compared with the Co-Au-Pd/rGO composite and Co-Au-Pd NPs. The Co-Au-Pd/DNA–rGO composite exhibited the highest activity compared to other catalysts and order of activity is Co-Au-Pd < Co-Au-Pd/rGO < Co-Au-Pd/DNA–rGO. Additionally no gas was generated from aqueous FA solution in the presence of DNA or the DNA–GO composite thereby suggesting that DNA and DNA–GO serve as a template and support, respectively, for the growth of Co-Au-Pd NPs, and not as catalysts, for FA dehydrogenation.

We have prepared a high-performance palladium silica nanosphere (20–35 nm) catalyst using $Pd(NH_3)_4Cl_2$ as precursor in a polyoxyethylene-nonylphenyl ether/cyclohexane reversed micelle system followed by $NaBH_4$ reduction.[108] Pd NPs supported on silica nanospheres (Pd/SiO_2) were prepared by the conventional impregnation of $Pd(NH_3)_4Cl_2$ precursor to silica nanospheres, which were prepared using a similar reversed micelle system without Pd precursor, followed by $NaBH_4$ reduction. The as-synthesized $Pd@SiO_2$ and Pd/SiO_2 catalysts have high catalytic activities than Pd NPs supported on commercial silica at convenient temperature. Remarkably, it was observed that the interactions of the Pd nanoparticles with surface groups of silica support are important for the catalytic performance. The strong cooperative effects from surface molecular groups on silica to the metal surface, that is, a strong metal–molecular support interaction (SMMSI), might bring new opportunities in the development of high-performance heterogeneous catalysts from inactive or less active metal catalyst systems.

Cai *et al.* synthesized Pd nanoparticles immobilized on mesoporous carbon nitride (Pd@CN) as highly efficient Mott–Schottky photocatalyst for dehydrogenation of formic acid.[109] The exceptional catalytic performance of catalyst was due to the enhanced electron enrichment of the Pd nanoparticles through charge transfer operating at the interface of the Mott–Schottky contact. Under similar operating conditions, the catalytic performance of Pd@CN is orders of magnitudes higher than that of similar Pd@carbon catalysts. Nanostructured carbon nitride acted both as the stabilizer and as semiconducting support for coupling of metal NPs to form the required rectifying Mott–Schottky nano-heterojunctions.

A basic resin bearing $-N(CH_3)_2$ functional groups within its macro-reticular structure performed as an efficient organic support for the active Pd nanoparticles responsible for the production of high-quality H_2 *via* formic acid (HCOOH) decomposition at convenient temperature (Fig. 5).[110] Physicochemical characterization as well as the kinetic isotope effect (KIE) revealed that not only the formation of small Pd NPs but also cooperative action by the $-N(CH_3)_2$ groups within the resins play crucial roles in achieving efficient catalytic performances. In addition to the advantages such as simple workup procedure, additives free, and superior catalytic activity compared with the conventional inorganic supports, this catalytic system can suppress unfavorable CO formation of <5 ppm, which makes it an ideal hydrogen vector in terms of potential industrial application for PEMFCs. Moreover, the basic resin support also provided Pd–Ag nanocatalyst from an aqueous solution of mixture of $PdCl_2$ and $AgNO_3$. The catalytic activities in the H_2 production from formic acid decomposition were strongly dependent on the presence of Ag atoms and were shown to perform significantly better than the pure Pd and Ag catalysts.

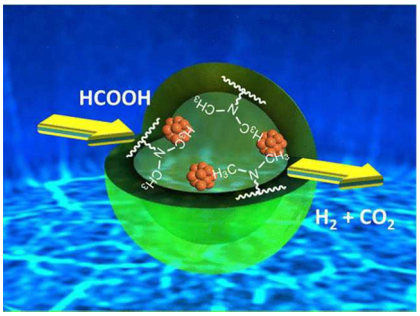

Fig. 5 Model of Pd nanoparticles supported on basic resin bearing $-N(CH_3)_2$ functional groups within its macroreticular structure. Reprinted with permission from ref. 110. Copyright 2013 American Chemical Society.

Highly dispersed Pd nanoparticles (NPs) deposited on nanoporous carbon MSC-30 have been synthesized using a sodium hydroxide-assisted reduction approach.[111] Use of NaOH during the formation and growth of particles resulted well-dispersed ultrafine Pd NPs on MSC-30. The combination of metal-support interaction and high dispersion of NPs

significantly enhanced the performance of the resulted catalyst. This catalyst exhibited 100% H_2 selectivity and very high activity (TOF = 2623 h^{-1}) for heterogeneously catalyzed decomposition of FA at 323 K. The activity of prepared catalyst was comparable to those acquired from the most active homogeneous catalysts as well as heterogeneous catalysts under ambient conditions.

Xu and co-workers reported synthesis of bimetallic Au-Pd NPs immobilized in mesoporous metal-organic framework (MOF) MIL-101 (Pore sizes = 2.9-3.4 nm and window sizes = 1.2-1.4 nm) as efficient catalysts for decomposition of formic acid towards generation of hydrogen.[112] Because of its ordered pore, small window and hybrid pore surface, MIL-101 facilitates the encapsulation of metal NPs and the adsorption of formic acid inside the pores. MIL-101 have coordinatively unsaturated Cr^{3+} centres. In order to improve the interactions between the metal precursors and the MIL-101 support, ED-MIL-101 has been prepared by grafting MIL-101 with electron-rich functional group ethylenediamine (ED). ED-MIL-101 exhibited improved immobilization of small metal NPs. Among the resulting bimetallic Au-Pd NPs immobilized in the MOFs Au-Pd/MIL-101 and Au-Pd/ED-MIL-101, represents the first highly active MOF-immobilized metal catalysts for the complete conversion of formic acid to hydrogen at convenient temperature.

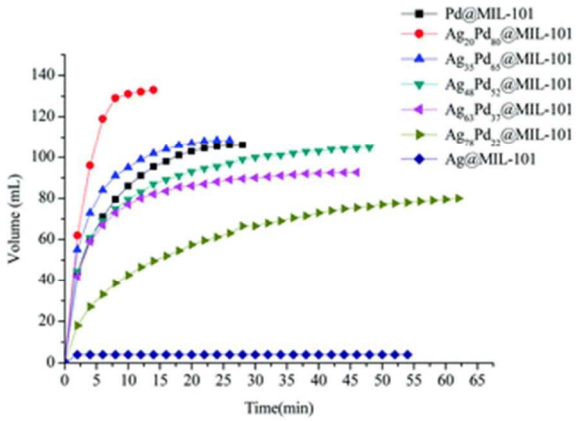

Fig. 6 Hydrogen generation from HCOOH in the presence of different catalysts: $Ag_{20}Pd_{80}$@MIL-101; $Ag_{35}Pd_{65}$@MIL-101; $Ag_{48}Pd_{52}$@MIL-101; $Ag_{63}Pd_{37}$@MIL-101; $Ag_{78}Pd_{22}$@MIL-101; Ag@MIL-101; Pd@MIL-101 at 353 K. Reprinted with permission from ref. 113. Copyright 2013 Royal Society of Chemistry.

Dai *et al.* investigated the activity of bimetallic Ag-Pd nanoparticles immobilized into MIL-101, for catalytic dehydrogenation of formic acid.[113] Among all the AgPd@MIL-101 catalysts with different compositions of Ag and Pd (Ag@MIL-101, $Ag_{78}Pd_{22}$@MIL-101, $Ag_{63}Pd_{37}$@MIL-101, $Ag_{48}Pd_{52}$@MIL-101, $Ag_{35}Pd_{65}$@MIL-101, $Ag_{20}Pd_{80}$@MIL-101 and Pd@MIL-101), the $Ag_{20}Pd_{80}$@MIL-101 catalyst exhibited the highest catalytic activity for the conversion of formic acid to high-quality hydrogen at 353 K with a TOF value of 848 h^{-1}, which is among the highest values reported at 353 K (Fig. 6).

In another report, Yamashita and co-workers used photocatalytically active metal-organic framework MIL-125 and its amine-functionalized equivalent NH_2-MIL-125 to immobilize Pd NPs by photo-assisted and ion exchange deposition methods.[114] Pd-NH_2-MIL-125 catalyst showed high catalytic activity for H_2 generation from FA at ambient temperature (TOF = 214 h^{-1} at 305 K) in comparison to Pd-MIL-125 and to the other titanium-based porous materials. The main factors responsible for the high catalytic performance were the basic functionalization of the MOF and small NPs sizes. In addition, the photo-assisted deposition method was found to be a more effective method for producing small and highly dispersed NPs within the MOF structure.

Zhang and co-workers synthesized well-dispersed Pd-Ni nanocatalysts grown on a graphene nanosheet-carbon black (GNs–CB) composite support to combine the advantages of GNs and CB.[115] Unexpectedly, Pd-Ni NCs loaded on GNs–CB exhibited higher catalytic performance for FA decomposition at room temperature in aqueous media than on Pd or Ni alone. Furthermore, Pd is employed to replace the surface Ni of Pd-Ni NCs toward a novel Pd-Ni@Pd catalyst to further improve the catalytic activity and stability. The use of GNs–CB as a new kind of carbon support to disperse, anchor, and further promote nanocatalysts with active components would undoubtedly assist long-term endeavours to further optimize and enhance the catalytic efficacy of catalysts in the development of FA as a hydrogen-storage material.

There are few reports for the formic acid decomposition by Au NPs based heterogeneous catalysts. First report on Au NPs based heterogeneous catalysts for formic acid dehydrogenation in gas phase at ambient temperatures have been reported by Ojeda and Iglesia in 2009.[89] Well-dispersed Au species immobilized on Al_2O_3 exhibited decomposition of HCOOH with metal-time yields (rates per Au atom) larger than on Pt clusters supported on Al_2O_3 at 353 K. HCOOH dehydrogenation proceeds *via* either a H-assisted formate decomposition mechanism or *via* sequential cleavage of O-H and C-H bonds and H-atom recombination on isolated sites.

First work of liquid phase dehydrogenation of formic acid by monometallic Au NPs based catalyst was reported by Xu and co-workers.[116] Monometallic gold nanoparticles encapsulated in amine functionalized silica nanospheres, acted as a high-performance catalyst for hydrogen generation from aqueous formic acid. It was observed that the unsupported or silica-supported gold NPs without amine functional group are inactive for FA dehydrogenation reaction. Hence, the presence of amine in the silica sphere is important for the activity of gold nanoparticles due to strong metal–molecular support interaction (SMMSI).

Bi *et al.* demonstrated mild and selective dehydrogenation of FA/amine mixtures using ultradispersed sub-nanometric gold NPs on acid-tolerant ZrO_2 as catalysts.[117] The catalytic reactions, proceed efficiently and selectively under ambient conditions, without the generation of any unwanted byproduct, such as CO, and with high TOFs/TONs. A unimolecular mechanism involving unique amine-assisted formate decomposition at the Au–ZrO_2 interface is supported by the exclusive formation of HD and the primary kinetic isotope

effects measured from HCOOD or DCOOH dehydrogenation (Fig. 7). Exceptional activity of sub-nanometric Au toward FA activation promises a new area of gold research by a fine-tuning of the dispersed Au clusters at the sub-nano level.

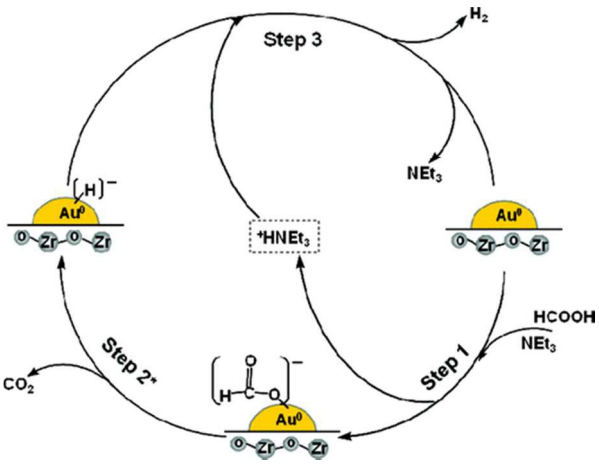

Fig. 7 Possible reaction pathway for hydrogen evolution from the 5:2 FA-NEt_3 azeotropic mixture system over the Au/ZrO_2 NCs catalyst. Reprinted with permission from ref. 117. Copyright 2012 American Chemical Society.

The activities of Pt catalysts on carbon nanofibers with different nitrogen contents were compared for hydrogen production by formic acid decomposition.[118] The catalysts contained a fraction of Pt clusters with a mean size of 1.0–2.3 nm and possibly a considerable fraction of Pt clusters with a diameter of less than 0.75 nm that were invisible by transmission electron microscopy (TEM). The activities of N-doped catalysts with low Pt contents (⩽1 wt%) were 10 times higher than the activities of undoped catalysts. The N-doped catalysts demonstrated an improved selectivity to hydrogen and an increased resistance to CO inhibition. However, they were inactive for ethylene hydrogenation. These results are explained by the presence of electron-deficient, two-dimensional sub-nm sized Pt clusters stabilized by pyridyl nitrogen on vacancy sites. In accordance, the Pt-$4f_{7/2}$ binding energies measured by X-ray photoelectron spectroscopy were 0.6 eV higher for the N-doped samples than for the undoped ones.

Yurderi *et al.* synthesized trimetallic Pd-Ni-Ag nanoparticles with different ratios of metals as well as its bi-metallic (Pd-Ni, Ni-Ag and Pd-Ag) and mono-metallic (Pd, Ni and Ag) counterparts supported on activated carbon by simple and reproducible wet-impregnation followed by simultaneous reduction method without using any stabilizer at room temperature.[119] All the prepared composites were employed as heterogeneous catalyst in the catalytic decomposition of formic acid under mild reaction conditions. It was found that Pd-Ni-Ag/C can catalyze the dehydrogenation of formic acid with high selectivity (~ 100%) and activity (TOF = 85 h^{-1}) at 323 K. More importantly, the exceptional stability of Pd-Ni-Ag nanoparticles against agglomeration, leaching and CO poisoning make Pd-Ni-Ag/C reusable catalyst in the formic acid dehydrogenation. Pd-Ni-Ag/C catalyst retained almost its inherent activity (> 94%) even at 5th reuse in the decomposition of formic acid with high selectivity (~ 100%) under ambient condition. The quantitative kinetic studies depending on the catalyst [Pd-Ni-Ag], substrate [FA] and promoter [SF] concentrations revealed that Pd-Ni-Ag/C catalyzed dehydrogenation of FA is first-order in catalyst concentration; half-order in promoter concentration and with respect to substrate concentration it appeared to be zero when [FA] < 0.140 M and half-order at higher concentrations. Pd-Ni-Ag/C catalyzed dehydrogenation of FA at different temperatures provided the activation parameters (E_a = 20.5 kJ/mol, $\Delta H^{\neq}$ = 17.8 kJ/mol, $\Delta S^{\neq}$ = -190 J/mol.K) and suggested the associative mechanism for the Pd-Ni-Ag/C catalyzed dehydrogenation of FA.

Recently, a potential boron-doped Pd nanocatalyst (Pd-B/C) was reported to enhance the hydrogen generation at room temperature from aqueous formic acid–formate solutions at a record high rate.[120] Pd/C and Pd-B/C catalysts with a Pd loading of 5 wt% were synthesized through wet chemical reduction of $NaBH_4$ and dimethylamine borane (DMAB), respectively. To exclude any boron doping, HCOONa was also used as the reducing agent to synthesize Pd/C-HCOONa. Catalytic studies suggested only a slightly higher gas production rate by Pd/C-$NaBH_4$ than on Pd/C-HCOONa (Fig. 8). In contrast, the gas production rate was nearly doubled on Pd-B/C as compared to the other two catalysts at a given mass of Pd. Present Pd−B/C catalyst show superior catalytic activity, compared to the TOF values reported so far for various Pd-based catalysts at room temperature.

Highly sensitive attenuated total reflection infrared spectroscopy (ATR-IR) was used to monitor dynamically the interfacial species on Pd-B/C or Pd/C in FA-SF solutions to provide a molecular-level understanding of different activities of the examined catalysts. ATR-IR spectroscopy revealed that the superior activity of Pd-B/C is related to an apparently impeded CO_{ad} (Adsorbed CO) accumulation on the surface of Pd-B/C catalyst. This work demonstrated that developing new anti-CO poisoning catalysts coupled with sensitive interfacial analysis is an effective way toward rational design of cost-effective catalysts for better hydrogen energy exploitation.

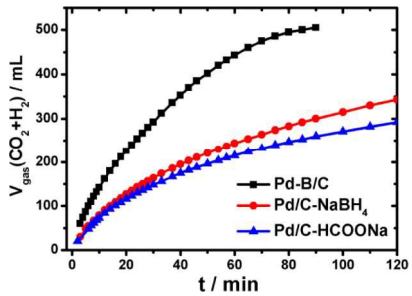

Fig. 8. Time-course of reforming gas generation from 10 mL solution of 1.1 M FA + 0.8 M SF in the presence of 100 mg of Pd based/C (5 wt% Pd) catalysts at 303 K under ambient atmosphere. Reprinted with permission from ref. 120. Copyright 2014 American Chemical Society.

Reversible, carbon dioxide mediated chemical hydrogen storage was first demonstrated using a heterogeneous Pd catalyst supported on mesoporous graphitic carbon nitride (Pd/mpg-C_3N_4).[121] The Pd nanoparticles are uniformly dispersed onto the mpg-C_3N_4 with an average size of 1.7 nm without any agglomeration and further exhibited superior activity for the dehydrogenation of formic acid with a turnover frequency of 144 h^{-1} even in the absence of external bases at room temperature. From DFT studies, it was confirmed that basic sites located at the mpg-C_3N_4 support play synergetic roles in stabilizing reduced Pd nanoparticles without any surfactant as well as in initiating H_2-release by deprotonation of formic acid. These potential interactions were further confirmed by X-ray absorption near edge structure (XANES). Along with dehydrogenation, Pd/mpg-C_3N_4 also proved to catalyze the regeneration of formic acid *via* CO_2 hydrogenation. The governing factors for CO_2 hydrogenation were further elucidated to increase the quantity of the desired formic acid with high selectivity.

Beller and co-workers carried out detail theoretical study for formic acid decomposition on various metal surfaces {such as Ni(111), Ni (211), Pd(111), Pd (211), Pt(111) and Pt(211)}, metal oxides (Such as TiO_2, MgO, ZnO and NiO) and Molybdenum carbide (β-Mo_2C(101)).[122-125] A common pathway observed for selective decomposition of formic acid to CO_2 and H_2 is shown in scheme 4. The formate route (HCOOH → HCOO + H) plays the dominating role in formic acid decomposition; and the rate-determining step is the dissociation of formate into surface CO_2 and H (HCOO → CO_2 + H). The most stable adsorption configuration of formate (HCO_2) has the bidentate bridging structure with its two oxygen atoms (C–O) at atop sites.

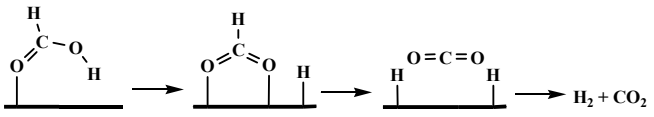

Scheme 4. General mechanism of formic acid decomposition over various surfaces through formate route.

Further works are required to develop an efficient system for hydrogen release from formic acid using heterogeneous catalyst owing to selectivity problems induced by the high reaction temperatures for heterogeneous catalytic reaction.

3. Formic Acid Production

Formic acid is an important platform chemical for the synthesis of diverse organic substances. In nature, FA is found in the venom of ants[28] and is occurring as component of the atmosphere due primarily to forest emissions.[126,127] Chemically it can be prepared by various processes. Most common industrial process is combination of methanol and carbon monoxide in the presence of a strong base at elevated pressure (40 atm) and temperature (353 K) for the preparation of methyl formate, followed by hydrolysis of the methyl formate to formic acid.[128]

$$CH_3OH + CO \rightarrow CH_3COOH \quad (7)$$

$$CH_3COOH + H_2O \rightarrow HCO_2H + CH_3OH \quad (8)$$

The established BASF technology is based on the use of methanol and CO.[129]

$$CH_3OH + CO \rightarrow CH_3OCHO \quad (9)$$

$$CH_3OCHO + H_2O \rightarrow CH_3OH + HCO_2H \quad (10)$$

Formally the net reaction is

$$H_2O + CO \rightarrow HCO_2H \quad (11)$$

An issue is the separation of formic acid from the reaction mixture. Other methods for the synthesis of FA are as a by-product of acetic acid production, CO_2 hydrogenation, oxidation of biomass, biosynthesis by reduction of carbon dioxide catalyzed by the enzyme formate dehydrogenase.[130,131] In this section, we will discuss in detail the different methods for formic acid production with major focus on CO_2 hydrogenation. Carbon dioxide, a major byproduct of FA decomposition either chemically or electrochemically and last product of any organic compound burnt in air, is a major green house gas. Utilization of this green house gas as a source for formic acid is not only a smart step to establish FA as a renewable energy but may help to reduce environmental deterioration.

3.1 Oxidation of biomass

Production of formic acid from biomass offers a mild and sustainable way to produce H_2.[132] Many researchers have studied the production of FA from biomasses (carbohydrates) using thermal cracking,[133] SCW/H_2O_2,[134] $Fe_2(SO_4)_3/O_2$ or $CuSO_4/O_2$[135,136] and OH^-/H_2O_2[137] etc. Wasserscheid and co-workers had performed a systematic study for selective oxidation of carbohydrate-based biomass to formic acid and CO_2 using Keggin-type $H_5PV_2Mo_{10}O_{40}$ polyoxometalate as catalyst under varying reaction conditions with different catalyst promoters.[138] In their first report, several water-soluble carbohydrate-based biomasses had been fully and selectively converted to formic acid and CO_2 by oxidation with molecular oxygen in aqueous solution under very mild conditions.[138] Glucose as substrate, their catalyst loading and temperature optimization (353 K, 30 bar O_2, 26 h) studies indicated that the characteristic FA yield at full conversion was 49% ± 2%. Interestingly, biogenic waste products, such as glycerol (from bio-diesel production), or xylane (from the hemicellulosic waste streams of paper manufacturing) were oxidized to FA in 40% and 33% yield, respectively. Using this catalyst even complex biomass mixtures, such as popular wood sawdust, were transformed to formic acid, giving 19 wt% yields (11% based on the carbon atoms in the feedstock) under non-optimized conditions.

Later, to optimize the reaction condition for water-insoluble biomass conversion to FA and CO_2, different additives (catalyst promoters) such as $CaCl_2$, H_3BO_3, $ZnCl_2$, LiCl and benzene/ toluene/ methane/ trifluoromethane/ camphor/ xylene/ chlorobenzene/ *p*-toluene sulphonic acid etc were used with polyoxometalate catalyst $H_5PV_2Mo_{10}O_{40}$ in water using oxygen (30 bar) as the oxidising agent at 363 K and reaction was monitored for 24 h.[139] Among all additives, *p*-toluenesulfonic acid acted as the best additive for transformation of feedstock like wood, waste paper, or even cyanobacteria to formic acid and CO_2 as the sole products. The produced FA can be separated from the aqueous reaction mixture by a simple extraction process and can be regarded as a hydrogen equivalent produced from biomass in a very robust process. The reaction achieved up to 53% yield in formic acid for xylan (hemicellulose) as the feedstock within 24 h at 363 K. Using this promoter, even third generation wet biomass such as algae could be efficiently converted to FA and CO_2 offering a very interesting path to the energetic use of these side products for future biodiesel production plants from algae.

In another work, Wasserscheid and co-workers modified the Keggin-type polyoxometalate catalyst and synthesized a series of different heteropolyacids (HPA) of the general type $H_{3+n}[PV_nMo_{12-n}O_{40}]$ (n = 0–6) (Scheme 5).[140] To confirm the reactivity, all the POM complexes were tested for conversion of glucose to FA using oxygen (at 30 bar) as oxidising agent. The higher V-substituted complexes (n = 2–6) showed superior activities than the lower V-substituted complexes (n = 0–1). Applying the optimized polyoxometalate catalyst system $H_8[PV_5Mo_7O_{40}]$ (HPA-5), a total FA-yield (with respect to carbon in the biogenic feedstock) of 60% for glucose within 8 h reaction time and 28% for cellulose within 24 h reaction time could be achieved at 363 K. The trend in the activity was explained on the basis of optic-al and electrochemical measurements which concluded that the formation of the pervanadyl species in higher V-substituted system was responsible for high activity of these HPA complexes. Mechanism comprises of two alternative ways for the dissociation of HPA-n. On one hand, before the oxidation reaction starts, the fully oxidized HPA-n with a reduction degree of m = 0 dissociates to free pervanadyl and the residual degenerated lacunary species. While, on the other hand, the fully reduced HPA-n after the substrate oxidation with a reduction degree of m = n dissociates to vanadyl (VO^{2+}) and the lacunary species.

Dissociation equilibria for HPA-n in aqueous solution

$$(\text{HPA-n})_{m=0} \rightleftharpoons (\text{HPA-n-1})_{m=0} + VO_2^+$$

$$(\text{HPA-n})_{m=n} \rightleftharpoons (\text{HPA-n-1})_{m=n-1} + VO^{2+}$$

Re-oxidation equilibria for HPA-n in aqueous solution

$$VO^{2+} + \text{HPA-n} + H_2O \rightleftharpoons VO_2^+ + \text{H(HPA-n)} + H^+$$

$$VO^{2+} + \text{(HPA-n-1)} + H^+ \rightleftharpoons \text{H(HPA-n)}$$

$$\text{Overall: } 4VO^{2+} + O_2 + 2H_2O \rightleftharpoons 4\,VO_2^+ + 4H^+$$

Scheme 5 Dissociation/re-oxidation equilibria for HPA-n in aqueous solution.

In an acidic solution, the free vanadyl (VO^{2+}) ion cannot be oxidised by molecular oxygen. Instead, the V^{4+} formed in the reaction returns into the heteropoly anion either by an electron transfer or by association with the lacunary species (HPA-n-1). Consequently, V^{4+} is re-oxidised by oxygen inside the HPA-n.

Li *et al*. also used the same catalyst and added H_2SO_4 as an additive to oxidize cellulose to get FA with 28% yield at 443 K and the cellulose got completely converted in 9 h. The increase in temperature and acidity (by adding H_2SO_4) increased the FA yield, and the time was shortened to 9 h. Under modified reaction condition, the conversion of glucose to formic acid could be achieved up to 52% yield within 3 h using 5 mol% of $H_5PV_2Mo_{10}O_{40}$ at 373 K using air as the oxidant.[141] Han *et al.* prepared three phosphovanadomolybdic acids with different contents of vanadium, namely $H_4PVMo_{11}O_{40}$, $H_5PV_2Mo_{10}O_{40}$ and $H_6PMo_9V_3O_{40}$ and three Keggin-type HPA catalysts including two V-free HPAs ($H_3PW_{12}O_{40}$ and $H_3PMo_{12}O_{40}$) and one phosphovanadotungstic acid ($H_5PV_2W_{12}O_{40}$), and evaluated their catalytic performance for the conversion of cellulose.[142] Although relatively low temperature (~373 K) was used to convert soluble carbohydrates, a higher reaction temperature (> 423 K) was essential for effective conversion of water-insoluble biomass (e.g. cellulose) with HPAs. $H_4PVMo_{11}O_{40}$ acts as the most efficient catalyst capable of converting varieties of biomass-derived substrates to formic acid and acetic acid with high selectivity in aqueous medium and oxygen atmosphere. Under optimized reaction conditions, $H_4PVMo_{11}O_{40}$ gave exceptionally high yield of formic acid (67.8%) from cellulose.

Recently, Liu *et al*. observed that heteropolyanion-based ionic liquids with $-SO_3H$ functionalized cations and $PMo_{11}VO_{40}^{4-}$ anions showed enhanced activity for catalysing cellulose conversion to FA in the presence of oxygen in water compared to $H_4PMo_{11}VO_{40}$.[143] Investigation of the possible pathway of FA production from cellulose was indicated that heteropolyanion-based ionic liquids served as bifunctional catalysts with cations catalysing the cellulose hydrolysis to glucose and anions catalysing glucose oxidation to FA. Optimization with different as prepared ionic liquid catalysts resulted high efficiency for FA production from cellulose conversion, giving a high FA yield over 50% and a high FA concentration of ~10% in aqueous solution at 453 K and in an oxygen pressure of 1.0 MPa.

Marsh and co-workers developed a catalytic process for efficient production of FA from common carbohydrates *via* VO_2^+ formed by dissolving sodium metavanadate in acidic water. The hydrolysis reaction decomposed the polymerized structures of polysaccharides to produce monosaccharides, which were readily oxidized to FA under catalysis of VO_2^+. Typically, formic acid mole yields were 64.9% from cellulose and 63.5% from xylan (hemicellulose) at 433 K.[144] Wang and co-workers used cheaper and less toxic vanadium salt, $VOSO_4$

as high-performance catalyst for the transformations of glucose and cellulose into either formic acid or lactic acid (LA) by simply tuning the reaction atmosphere from O_2 to N_2. The catalytic reaction proceeds through the isomerization of glucose to fructose, which subsequently underwent retro-aldol fragmentation to two trioses, that is, glyceraldehyde and 1,3-dihydroxyacetone**.** The isomerization of these trioses under N_2 led to the formation of lactic acid. The oxidative cleavage of C-C bonds in the intermediates caused by the redox conversion of VO_2^+/VO^{2+} under aerobic conditions resulted in formic acid and CO_2. Addition of an alcohol suppresses the formation of CO_2 and enhances the formic acid yield significantly to 70–75 %.[145]

From all the observations by different groups, it can be concluded that biomass could be converted to formic acid by vanadyl species (VO_2^+/VO^{2+}) or heteropolyacids (HPA) containing vanadyl ions. These catalysts work as bifunctional catalyst for conversion of polysaccharides to monosaccharide as well as selective conversion of the generated monosaccharides to formic acid and CO_2 under acidic condition using air or oxygen as oxidant.

Besides vanadyl containing catalysts, some people reported production of FA from bio-mass in presence of other catalysts and some additives.[146-148] Gao *et al.* successfully produced FA with 22% yield from pretreated cellulose under hydrothermal condition at 483 K for 30 h.[146] A high yield of 75% FA was produced by Jin *et al.* at 523 K using 120% H_2O_2 from glucose.[147] Chaudhary *et al.* designed a Cu catalyst suitable for the conversion of biomass to lactic acid (LA) and formic acid.[148] They synthesized magnesia supported copper catalyst by hydrothermal methodology using CTAB as capping agent (denoted as Cu-CTAB/MgO). Interestingly, this catalyst boosted the yields of LA and FA dramatically from sugars with decreasing reaction temperature from 523 K to 393 K. Glucose can be converted to lactic acid or formic acid depending on different additives. Lactic acid with the yield of 70% was produced in the presence of NaOH while FA produced in the presence of H_2O_2 were achieved from glucose at 393 K in water using Cu-CTAB/MgO catalyst, which could be recycled without any significant loss of activity. The catalyst was also found to exhibit excellent activity for transformation of other sugars.

Besides all efforts, complete and selective conversion of biomass to formic acid and CO_2 is still a challenging task and further work is required to replace the harsh reaction conditions with mild conditions.

3.2 CO_2 hydrogenation

Energy is the most indispensable element of our daily lives, which comes mostly from fossil fuels. Apart from the limited source of these non-renewable fossil fuels, our dependency on them has caused serious environmental concerns, such as green house gases (CO_2) as well as other toxic pollutants. Best way to overcome this problem is the use of CO_2 to make high value chemicals. Extensive researches have been carried out on utilization of carbon dioxide to prepare high value chemicals such as formic acid, formaldehydes, methanol, methane, other long chain organics and in synthetic chemistry to get different products at ambient conditions.[129,149] Conversion of CO_2 to useful chemicals is of significant importance not only due to reductions in greenhouse gases but to build an energy infrastructure that uses methanol or formic acid etc.[70,150-153] Unlike conversion to formic acid, conversion of CO_2 to formaldehydes, methanol or methane requires harsh conditions which may deactivate catalysts, hence, these reduction processes are economically unfavourable.

Hydrogenation of CO_2 to formic acid is an important step to establish formic acid as a reversible hydrogen storage material. Several research works have been done in this field and those works are summarized in several excellent review articles as well as book chapters.[10,32,70,149-161] Hence, we are presenting here only the basic concept of conversion process and summarizing only some important recent researches on this topic.

3.2.1. Homogenous catalysts

Pioneer work on catalytic hydrogenation of CO_2 to formic acid has been reported by Inoue *et al.* in 1976.[129] The reaction was accelerated by adding small amounts of H_2O because ΔG value is negative in aqueous medium while positive in gaseous phase. Hence, reaction is favourable in aqueous medium. In addition, use of bases enhance the catalytic activity because basic additives, such as NaOH, $NaHCO_3$, Na_2CO_3 and amines, can absorb the generated proton and make the reaction thermodynamically more favourable (Eqs 8-10).

$$CO_2\,(g) + H_2\,(g) \rightarrow HCOOH\,(l) \qquad \Delta G = 32.9\ kJ\ mol^{-1} \quad (12)$$

$$CO_2\,(aq) + H_2\,(aq) \rightarrow HCOOH\,(aq) \quad \Delta G = -4.0\ kJ\ mol^{-1} \quad (13)$$

$$CO_2\,(aq) + H_2\,(aq) + NH_3\,(aq) \rightarrow HCOO^-\,(aq) + NH_4^+\,(aq) \qquad \Delta G = -9.5\ kJ\ mol^{-1} \quad (14)$$

Most of the complexes used to catalyze CO_2 hydrogenation are based on VIII transition metals such as Pd, Ni, Rh, Ru, and Ir. Among these catalysts, Rh, Ru, and most recently Ir complexes were found to be most effective. Recently, groups of Himeda and Fujita summarized homogeneous CO_2 hydrogenation to formate and methanol as an alternative to photo- and electrochemical CO_2 reduction with major emphasis on half-sandwich iridium catalyst based on proton responsive ligands.[161]

Yang *et al.* studied the reaction mechanisms for hydrogenation of carbon dioxide catalyzed by PNP-ligated (PNP = 2,6-*bis*(di-isopropylphosphinomethyl)pyridine) metal pincer complexes, $(PNP)MH_n$ (M = Ir, Fe and Co) computationally by using the density functional theory (DFT).[162] Iridium is a recently reported high efficiency catalyst for the formation of formic acid from H_2 and CO_2.[163] Fe and Co metal complexes would be use as low-cost non-noble metal catalyst for CO_2 reduction.

Using rhodium-phosphine complex, $[RhCl(mtppms)_3]$ (mtppms = monosulfonated triphenylphosphine) as catalyst, free formic acid was produced in hydrogenation of carbon

dioxide dissolved in aqueous sodium formate solutions under H_2 and CO_2 pressure with the water-soluble concentration of sodium formate.[164] Total gas pressure and the pressure ratio of H_2 to CO_2 were the most important factors for production of HCOOH. Up to 0.13 M concentration of HCOOH was achieved, while there was negligible formic acid production in the absence of sodium formate.

Himeda *et al.* reported the interconversion between formic acid and H_2/CO_2 using half-sandwich rhodium and ruthenium catalysts with 4,4'-dihydroxy-2,2'-bipyridine (DHBP).[165] In the hydrogenation of CO_2/bicarbonate to formate under basic conditions, activations of the catalysts were caused by the electronic effect of oxyanions generated by deprotonation of the hydroxyl group. The turnover frequencies of these catalysts increased 65- and 8-fold, respectively, compared to the corresponding unsubstituted bipyridine complexes. The rhodium-DHBP catalyst showed high activity without CO contamination in a relatively wide pH range. These catalytic systems are extremely useful for H_2 storage material by combining CO_2 hydrogenation with formic acid decomposition.

Maenaka *et al.* synthesized [C,N] cyclometalated organoiridium complex, $[Ir^{III}(Cp^*)(4\text{-}(1H\text{-pyrazol-1-yl-}\kappa N^2)\text{benzoic acid-}\kappa C^3)(H_2O)]_2SO_4$, as an efficient catalyst for interconversion between hydrogen and formic acid in water at ambient temperature and pressure for both directions depending on pH.[166] Hydrogenation of carbon dioxide occurs in the presence of a catalytic amount of Ir complex under an atmospheric pressure of H_2 and CO_2 in weakly basic water (pH 7.5) at room temperature, whereas formic acid efficiently decomposes to afford H_2 and CO_2 in acidic water (pH 2.8).

Wesselbaum *et al.* presented a new idea that allows the continuous-flow hydrogenation of supercritical CO_2 ($scCO_2$) with integrated product separation from an immobilized catalyst and stabilizing base to produce pure formic acid in a single processing unit.[167] The concept is based on a biphasic reaction system consisting of $scCO_2$ as mobile phase and an ionic liquid as stationary phase containing the catalyst and a nonvolatile base (Scheme 6). The pure HCO_2H that is free of any cross-contamination can be obtained without interrupting the working catalyst inside the reactor by this method.

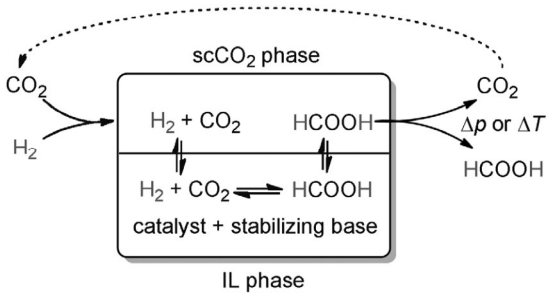

Scheme 6. Process for the direct continuous-flow hydrogenation of CO_2 to free formic acid based on a two-phase system with $scCO_2$ as extractive mobile phase and an ionic liquid (IL) as stationary phase containing the catalyst and the stabilizing base. Reprinted with permission from ref. 167. Copyright 2012 Wiley-VCH.

Huff *et al.* have synthesized the Ruthenium pincer complex Ru(PNN)CO(H) (PNN = 6-(di-tert-butylphosphinomethylene)-2-(N,N-diethylaminomethyl)-1,6-dihydropyridine) which is an efficient catalyst for the hydrogenation of carbon dioxide to formate. Stoichiometric studies are presented that support the feasibility of the individual steps in a proposed catalytic cycle for this transformation.[168] They explored the influence of base and solvents on catalytic performance. Under optimized conditions (using diglyme as the solvent and potassium carbonate as the base) up to 23,000 turnovers of formate and a turnover frequency of up to 2,200 h^{-1} was achieved.

The activity of homogeneous ruthenium(II)-1,2-*bis*(diphenylphosphino)ethane as a catalyst was studied for the equilibrium position in formic acid/amine-CO_2 systems as a function of pressure and temperature under isochoric conditions.[169] It was found that Ru catalyst was active for both that is, in formic acid cleavage producing pure hydrogen and CO_2, as well as in carbon dioxide hydrogenation under basic conditions. High yields of formic acid dehydrogenation into H_2 and CO_2 are favoured by low gas pressures and/or high temperatures, and H_2 uptake is possible at elevated H_2-CO_2 pressures.

Recently, the direct hydrogenation of CO_2 into formic acid using a homogeneous ruthenium catalyst has been studied by Moret *et al.* in aqueous solution and in dimethyl sulphoxide (DMSO) without any additives.[170] In water, at 313 K, 0.2 M formic acid can be obtained under 200 bar, however, in DMSO the same catalyst affords 1.9 M formic acid. In both solvents the catalysts can be reused multiple times without a decrease in activity. Worldwide demand for formic acid continues to grow, especially in the context of a renewable energy hydrogen carrier, and its production from CO_2 without base, *via* the direct catalytic carbon dioxide hydrogenation, is considerably more sustainable than the existing routes.

Drake *et al.* have investigated the role of various common inorganic salts to increase in productivity for the hydrogenation of CO_2 to formic acid in presence of various catalysts.[171] Among the various salts, $KHCO_3$ acted as a best promoter for hydrogenation of CO_2. Selectivity for formic acid production catalyzed by $RuCl_2(PPh_3)(p\text{-cymene})$ could be increased by 84% to 140% depending on the amount of $KHCO_3$. The effect was general for other noble-metal catalysts and for one of the most efficient non-noble-metal hydrogenation catalysts shown in Fig. 9. Mechanistic experiments revealed that the reaction likely proceeds *via* the formation of a metal–carbonate species.

Hsu *et al.* have reported the use of a Ru catalyst [(PNNP)(acetonitrile)Ru^{II}] for the efficient and reversible reduction of CO_2 to formic acid in the presence of DBU as a base.[172] At a catalyst loading of only 0.075 mol% both the reduction using H_2 pressure as well as the decomposition of the formic acid adduct under pressure-free conditions were established.

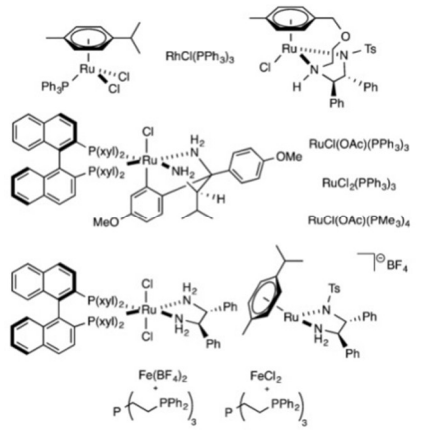

Fig. 9 Catalysts used for hydrogenation of CO_2. Reprinted with permission from ref. 171. Copyright 2013 American Chemical Society.

The homogeneously catalyzed hydrogenation of carbon dioxide to formic acid and its derivates has been well studied. Recently, an increase in product formation was achieved by further development of the homogeneous catalysts. Currently, iridium based catalysts offer the highest catalytic activity known in the hydrogenation of carbon dioxide. Here we summarized various catalyst systems for CO_2 hydrogenation to formic acid (Table 3) as reported in a recently book chapter by Behr *et al*.[38]

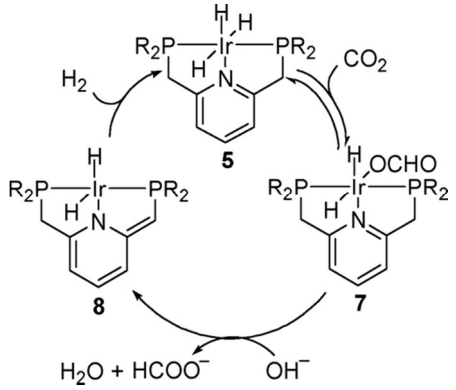

Fig 10. Plausible Mechanism for Hydrogenation of CO_2 Using Iridium trihydride complex. Reprinted with permission from ref. 173. Copyright 2011 American Chemical Society.

Some catalysts are found to be active for reversible CO_2 hydrogenation as well as formic acid dehydrogenation by varying the reaction condition.[163,173] These systems hold promise for the development of a practical H_2 storage technology based on the reversible catalytic hydrogenation of CO_2. Nozaki and co-workers reported highly active catalytic hydrogenation of carbon dioxide to form formic acid salts and dehydrogenation of formic acid salt using a PNP-ligated iridium(III) trihydride complex (Fig. 10). Hydrogenation of carbon dioxide using this PNP-ligated iridium(III) trihydride complex afforded potassium formate in aqueous KOH solution with a TOF of 150 000 h^{-1} and a TON of 3500000, both of the values being the highest ever reported.[163,173] In the presence of triethanolamine as the base, both CO_2 hydrogenation (TON 29000, TOF 14000 h^{-1} at 5.0 MPa at 297K) and FA dehydrogenation (TON 4900, TOF 1000 h^{-1} at 333 K) proceed at appreciable rate, showing that the iridium catalyst can be used for reversible hydrogen storage by changing the reaction condition only.

Pidko *et al.* reported highly efficient reversible hydrogenation of carbon dioxide to formates using a ruthenium PNP-pincer catalyst.[174] This catalyst has a very high activity for CO_2 hydrogenation and FA dehydrogenation. If used in combination with 1,8-diazabicyclo[5.4.0]undec-7-ene (DBU), catalyst allows the control of hydrogen liberation activity in a narrow temperature interval. H_2 capacity is dependent on the base strength, and strong bases are required to generate high acid-to-amine ratio at elevated temperature if the reaction times are short.

Besides the several works on noble-metal based catalysts, some non-precious-metal catalysts based on Fe,[70,175-179] Co,[180-182] Ni,[176,183] Cu,[184] Mo,[176] Ti[185] have also been investigated. Bellar and co-workers reported efficient, stable, and easy-to-synthesize non-noble metal complex iron(II)-fluoro-tris(2-(diphenylphosphino)phenyl)phosphino]tetrafluoroborate for the reduction of CO_2 and bicarbonates.[178] Catalytic hydrogenation of bicarbonates proceeded in good yields in with high catalyst productivity and activity (TON > 7500, TOF > 750 h^{-1}).

Beller and co-worker successfully utilized a cationic $Co(BF_4)_2{\cdot}6H_2O/PP_3$ catalyst systems for conversion of sodium bicarbonate/CO_2 to sodium formate (TON 687 at 353 K and 3877 at 393 K).[180] A cobalt based catalyst system for the production of formate from CO_2 and H_2 under ambient conditions has been synthesized by Jeletic *et al*.[181] The complex $Co(dmpe)_2H$ (dmpe = 1,2-*bis*(dimethylphosphino)ethane) catalyzes the hydrogenation of CO_2, with a TOF of 3400 h^{-1} at room temperature and 1 atm of 1:1 CO_2:H_2 (74000 h^{-1} at 20 atm) in thf. These results highlighted the value of fundamental thermodynamic properties in the rational design of catalysts. Himeda *et al.* reported new water-soluble pentamethylcyclopendadienyl cobalt(III) complexes with proton-responsive 4,4′- and 6,6′-dihydroxy-2,2′-bipyridine ligands as efficient catalysts for CO_2 hydrogenation to formate in aqueous bicarbonate media at moderate temperature under a total 4−5 MPa (CO_2:H_2 1:1) pressure.[182]

Several possible mechanisms are conceivable for CO_2 hydrogenation to formic acid which mainly involves insertion of CO_2 to M-H bond followed by elimination of FA. Insertion of carbon dioxide into the M–H bond is identical for all mechanisms in which carbon dioxide forms a metal formate complex via η^2-coordination and migration of hydrogen (Scheme 7).[38]

Table 3: Some homogeneous catalyst for selective CO_2 hydrogenation to formic acid and reaction conditions, Data obtained from ref. 38.

SN	Catalyst	Solvent	Base/Additive	T (K)	P CO_2/H_2 (bar)	Time (h)	TON (h^{-1})	TOF (h^{-1})
1	$[Ru(Cl_2bipy)_2(H_2O)_2]$ $[CF_3SO_3]_2$	EtOH	NEt_3	323	30/30	8	5000	625
2	$RuCl_2(PMe_3)_4$	$scCO_2$	NEt_3	323	120/80	47	7200	n.a.
3	$[RuCl(C_6Me_6)(DHphen)]Cl$	H_2O	KOH	393	30/30	24	15400	642
4	$RuCl(OAc)(PMe_3)_4$	$scCO_2$	NEt_3	323	120/70	0.3	31700	95000
5	$[RuCl_2(mTPPMS)_2]_2$	H_2O	$NaHCO_3$	353	35/60	0.03	320	9600
6	$RuH_2(PMe_3)_4$	$scCO_2$	NEt_3	323	120/85	1	1400	1400
7	$Ru_2(CO)_5(dppm)_2$	Acetone	NEt_3	RT	38/38	21	2160	103
8	$RuCl_3/PPh_3$	EtOH	NEt_3	333	60/60	5	200	40
9	$CpRu(CO)(\mu\text{-}dppm)Mo(CO)_2Cp$	Benzene	NEt_3	393	30/30	45	43	1
10	$TpRuH(PPh_3)(CH_3CN)$	THF	NEt_3	373	25/25	16	1815	113
11	$RuH_2(PPh_3)_4$	Benzene	NEt_3	RT	25/25	20	87	4
12	$RuH_2(PPh_3)_4$	Benzene	Na_2CO_3	373	25/25	4	169	42
13	$[(C_5H_4(CH_2)_3NMe_2)Ru(dppm)]BF_4$	THF	None	353	40/40	16	8	0.5
14	$[RuCl_2(CO)_2]n$	H_2O, *i*PrOH	NEt_3	353	27/81	0.3	400	1300
15	$RuCl_3$(aq)/dppbts	H_2O	$HNMe_2$	333	25/25	15	4980	n.a.
16	$K[RuCl(EDTA\text{-}H)Cl].2H_2O$	H_2O	None	313	17/3	0.5	n.a.	250
17	$RuCl_2(PTA_4)$	H_2O	$NaHCO_3$	353	0/60	n.a	n.a	807
18	$[(Cl_2bipy)_2Ru(H_2O)_2][CF_3SO_3]_2$	EtOH	NEt_3	423	30/30	8	5000	n.a.
19	$[(NHC)_2RuCl][PF_6]$	H_2O	KOH	473	20/20	75	23000	n.a.
20	$[(C_6Me_6)Ru(dhbipy)]$	H_2O	KOH	393	30/30	8	13620	4400
21	[(dppm)Ru(H)(Cl)]	H_2O	$NaHCO_3$	343	0/50	2	1374	687
22	$[RuCl_2(TPPMS)_2]_2$	H_2O	$NaHCO_3$	298	5/35	2	524	262
23	[Cp*Ru(DHphen)Cl]Cl	H_2O	KOH	393	30/30	24	15400	3600
24	$[(\eta^6\text{-arene})Ru(\eta^2\text{-N,O-L})(H_2O)]BF_4$	H_2O	NEt_3	373	50/50	10	400	n.a.
25	$RuH_2(PMe_3)_4$	$scCO_2$	NEt_3	323	120/80	3	1900	630
26	$RuH_2(PPh_3)_4$	DBF	TEtA	323	30/30	1	698	698
27	Rh(hfacac)(dcpb)	DMSO	NEt_3	298	20/20	5	n.a.	1335
28	$RhCl(TPPTS)_3$	H_2O	$NHMe_2$	RT	20/20	12	3439	n.a.
29	$[RhH(cod)]_4$/dppb	DMSO	NEt_3	RT	20/20	18	2200	375
30	$RhCl(TPPTS)_3$	H_2O	$NHMe_2$	354	20/20	0.5	n.a.	7260
31	$[RhCl(cod)]_2$/dippe	DMSO	NEt_3	297	40 total	18	205	11
32	$RhCl(PPh_3)_3$	benzene	Na_2CO_3	373	55/60	3	173	58
33	$[Rh(\eta^2\text{-CYPO})_2]BPh_4$	MeOH	NEt_3	328	25/25	7	1000	n.a
34	$RhCl_3/PPh_3$	H_2O	$NHMe_2$	323	10/10	10	2150	215
35	$[Rh(NBD)(PMe_2Ph)_3]BF_4$	THF	None	313	48/48	48	128	3
36	$RhCl(PPh_3)_3/PPh_3$	MeOH	NEt_3	298	40/20	20	2700	125
37	$RhCl_3$(aq)/dppbts	H_2O	$HNMe_2$	333	25/25	15	3910	n.a.
38	$[RhCl(cod)]_2$/dppb	DMSO	NEt_3	RT	20/20	22	1150	52
39	$RhCl(TPPTS)_3$	H_2O	NEt_3	296	20/20	n.a.	n.a.	1364
40	[Cp*Rh(DHphen)Cl]Cl	H_2O	KOH	353	20/20	32	2400	270
41	Rh(NO)(dcpe)	n.a.	DBU	323	1.5/1.5	16	106	n.a.
42	$[RhCl(mTPPMS)_3]$	H_2O	HCOONa	323	50/50	20	65	n.a.
43	$[RhCl(mTPPMS)_3]$	H_2O	$CaCO_3$	323	20/80	24	300	n.a.
44	[Cp*Ir(dhbipy)Cl]Cl	H_2O	KOH	393	30/30	57	42000	190000
45	[Cp*Ir(DHphen)Cl]Cl	H_2O	KOH	393	30/30	48	222000	33000
46	[Cp*IrCl(DHphen)]Cl	H_2O	KOH	393	30/30	10	21000	2100
47	$[(PNP)IrH_3]$	H_2O	KOH	393	30/30	48	3500000	73000
48	$[IrI_2(AcO)$(bis-NHC)]	H_2O	KOH	473	30/30	75	190000	n.a.
49	$PdCl_2$	H_2O	KOH	433	n.a./110	3	1580	530
50	$PdCl_2$	H_2O	KOH	513	40/106	3	340	n.a.
51	$Pd(dppe)_2$	Benzene	NEt_3	383	25/25	20	62	3
52	$Pd(dppe)_2$	Benzene	NaOH	RT	24/24	20	17	0.9
53	$PdCl_2[P(C_6H_5)_3]_2$	Benzene	NEt_3	RT	50/50	n.a.	15	n.a.
54	$FeCl_3$/dcpe	DMSO	DBU	323	60/40	7.5	113	15.1
55	$Fe(BF_4)_2{\cdot}6H_2O$, PP_3	MeOH	$NaHCO_3$	353	0/60	20	610	n.a.
56	$Co(BF_4)_2{\cdot}6H_2O$, PP_3	MeOH	$NaHCO_3$	353	0/60	20	3877	n.a
57	trans-[(tBu-PNP)Fe(H_2)(CO)]	H_2O	NaOH	393	3.33/6.66	5	788	n.a
58	$NiCl_2$(dcpe)	DMSO	DBU	323	160/40	216	4400	20
59	$Ni(dppe)_2$	Benzene	NEt_3	RT	25/25	20	7	0.4
60	$TiCl_4/Mg$	THF	None	RT	1/1	24	15	n.a.
61	$MoCl_3$/dcpe	DMSO	DBU	323	60/40	7.5	63	8

bipy = 2,2'-bipyridine, cod = cyclooctadiene, CYPO = $Cy_2PCH_2CH_2OCH_3$, DBF = dibutylformamide, DBU = 1,8-diazabicyclo[5.4.0]undec-7-ene, dcpb = $Cy_2P(CH2)_4PCy_2$, dcpe = 1,2-dicyclohexylphosphinoethane, dhbipy = 4,4'-dihydroxy-2,2'-bipyridine, DHphen = 4,7-dihydroxy-1,10-phenanthroline, dippe = 1,2-(diisopropylphosphino)ethane, dppb = 1,4-bis(diphenylphosphino)butane, dppbts = tetrasulfonated-1,4-bis(diphenylphosphino)butane, dppp = 1,3-bis(diphenylphosphino)propane, hfacac = hexafluoroacetylacetonate, mTPPMS = meta-monosulfonated triphenylphosphine, NBD = bicycle[2.2.1]hepta-2,5-diene, NHC = N-heterocyclic carbine, PP_3 = $[P(CH_2CH_2PPh_2)_3]$, PTA = 1,3,5-triaza-7-phosphaadamantane, TEtA = triethanolamine, Tp = hydrotris(pyrazolyl)borate, TPPMS = monosulfonated triphenylphosphine, TPPTS = trisulfonated triphenylphosphine

Theoretically, it is established that insertion can occur by M–H bond breaking based on the weak H–CO_2 interaction.[186-188] Elimination of formic acid can proceed *via* reductive elimination of formic acid, addition of hydrogen to the formate complex, direct hydrogenolysis of the M–O bond without previous oxidative addition to hydrogen or hydrolysis of the metal formate.[38,189-191]

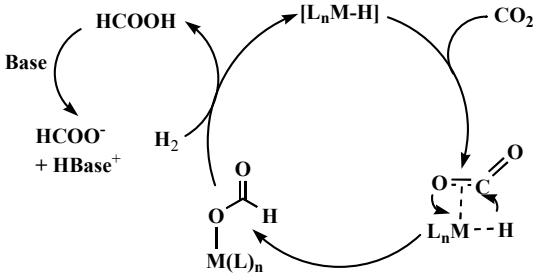

Scheme 7. General mechanism for the homogeneously catalyzed hydrogenation of CO_2 to FA.

3.2.2. Heterogeneous catalysts

Compared to homogeneous catalysts, there are only a few reports on CO_2 hydrogenation to formic acid over heterogeneous catalysts owing to the unfavorable reaction conditions and low chemoselectivity. For the first time, hydrogenation of CO_2 to formic acid was reported in 1935 using RANEY® nickel as catalyst under 200–400 bar hydrogen pressure and 353-423 K.[192] However, one equivalent of amine had to be added in order to shift the thermodynamic equilibrium towards the formation of the product formic acid.

Wiener *et al.* reported reduction of carbonates to formic acid under mild reaction conditions using Pd/C as catalyst.[193] However, the reaction could not achieve completeness due to the chemical equilibrium between carbonate and formate. Preti et *al.* examined the activity of some heterogeneous catalysts, such as iron powder, Raney nickel and Co, Cu, Ru, Rh, Pd, Ag, Ir, Pt and Au black, for the formation of formic acid by CO_2 hydrogenation.[194] Au black catalyses the CO_2 hydrogenation in the presence of neat NEt_3 to form HCOOH/NEt_3 adducts. Activity studies have been extended to commercially available aurolite (Mintek; 1 wt % Au/TiO_2, extrudates). Formic acid can be separated from HCOOH/NEt_3 with the help of high-boiling amine (n-$C_6H_{13})_3$N. When coupled with the catalytic HCOOH decomposition to CO-free hydrogen together with easily removable and reusable CO_2, these findings complete the chemical loop for the long-sought-after hydrogen storage with CO_2.

Hao *et al.* reported the preparation and application of heterogeneous supported ruthenium catalysts.[195] The catalysts were active in the synthesis of formic acid from the hydrogenation of carbon dioxide. Abundant hydroxyl groups, which interact with the ruthenium components, play an important role in the catalytic reactions. Highly dispersed ruthenium hydroxide species enhance the hydrogenation of CO_2, while crystalline RuO_2 species, which are formed during preparation of the catalyst, restrict the production of formic acid. Best activity of ruthenium hydroxide as a catalyst for the hydrogenation of CO_2 to formic acid was achieved over a γ-Al_2O_3 supported 2.0 wt% ruthenium catalyst, which is prepared in a solution of pH 12.8 with $NH_3 \cdot H_2O$ as a titration solvent.

A series of catalysts made of ruthenium loaded on γ-Al_2O_3 and γ-Al_2O_3 nanorods were studied for hydrogenation CO_2 to formic acid by Preti *et al.*[196] Among these catalysts, 2% Ru/Al (n) has highest activity. The excellent catalytic activity is related to the highly dispersed ruthenium species on the surface of support and abundant hydroxyl groups of the support.

A series of catalysts made of ruthenium loaded on γ-Al_2O_3 nanorods were prepared and their catalytic performances for hydrogenation CO_2 to formic acid have been studied by Na Liu *et al.*[197] The results revealed that the catalytic activity is determined by the structure of supported ruthenium oxide species. Optimal activity of catalyst for the hydrogenation of CO_2 to formic acid is achieved over a γ-Al_2O_3 nanorods supported 2.0 wt% ruthenium catalyst.

Peng *et al.* theoretically investigated the hydrogenation of CO_2 to formic acid on transition metal surfaces because it exhibit unique reactivity for hydrogenation reaction. They explored the potential of subsurface hydrogen for hydrogenating carbon dioxide on Ni(110).[198] A heterogeneous, mesoporous silica-tethered iridium catalyst (Ir-PN/SBA-15) containing a bidentate iminophosphine ligand is reported for the hydrogenation of CO_2 to formic acid in aqueous solution.[199] This catalyst is recyclable and exhibits high activities to formic acid production under mild conditions [333 K, 4.0 MPa total pressure (H_2/CO_2=1:1)].

The reaction mechanisms of hydrogenation of carbon dioxide to formic acid over Cu-alkoxide-functionalized metal organic framework (MOF) have been investigated theoretically.[200] The reaction can preceed *via* two different pathways, namely, concerted and stepwise mechanisms. In the concerted mechanism, the hydrogenation of CO_2 to formic acid occurs in a single step. It requires high activation energy of 67.2 kcal/mol. For the stepwise mechanism, the reaction begins with the hydrogen atom abstraction by CO_2 to form a formate intermediate. The intermediate then takes another hydrogen atom to form formic acid. The activation energies are calculated to be 24.2 and 18.3 kcal/mol for the first and second steps, respectively. Because of the smaller activation barriers associated with this pathway, it therefore seems to be more favoured than the concerted one.

Ruthenium complexes immobilized over amine-functionalized silica have been synthesized by an *in situ* synthetic approach.[201] The catalyst exhibits high activity (TOF = 1384 h^{-1}) with complete (100%) selectivity for CO_2 hydrogenation to formic acid. Immobilization of homogeneous catalysts offers practical advantages such as easy separation and recycling. The combination of a basic ionic liquid 1-(*N*,*N*-dimethylaminoethyl)-2,3-dimethylimidazolium

trifluoromethane-sulfonate ([mammim][OTf]) and a silica-supported ruthenium complex ("Si"–$(CH_2)_3$–$NH(CSCH_3)$–$RuCl_3$–PPh_3) found to catalyze CO_2 hydrogenation to formic acid with satisfactory activity and selectivity.[202] This immobilized catalyst catalyzes the hydrogenation of CO_2, with maximum TOF 103 h^{-1} at a total pressure of 18 bar (H_2 : CO_2 = 1 : 1) without loss in activity over 5 catalytic cycles.

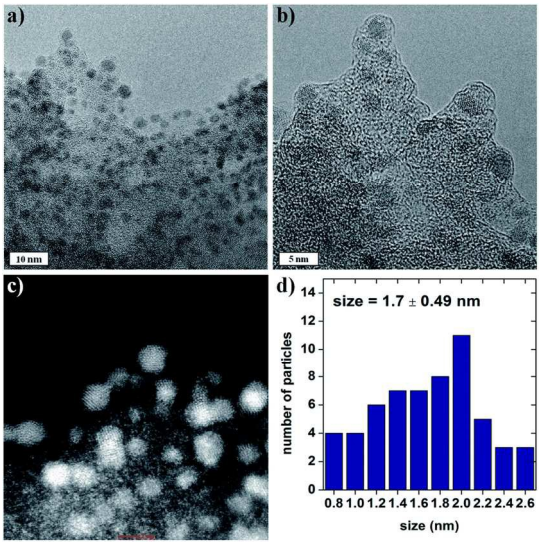

Fig. 11 HRTEM analyses: (a and b) images of Pd/mpg-C3N4, (c) HADDF-STEM image of Pd/mpg-C3N4, and (d) particle size distribution of Pd/mpg-C3N4. Reprinted with permission from ref. 121. Copyright 2014 Royal Society of Chemistry.

A reversible heterogeneous Pd catalyst (>3 nm) supported on mesoporous graphitic carbon nitride (Pd/mpg-C_3N_4) for interconversion of CO_2 and formic acid, has been synthesized by Lee *et al.* (Fig. 11).[121] This catalyst catalyze the formation of formic acid *via* CO_2 hydrogenation along with dehydrogenation of formic acid with a turnover frequency of 144 h^{-1} even in the absence of external bases at room temperature. The basic sites of the support could also induce initial interaction with CO_2 for the synthesis of FA. The governing factors of CO_2 hydrogenation are further elucidated to increase the quantity of the desired formic acid with high selectivity.

3.3. Photochemical and enzymatic reductions of CO_2 to formic acid

CO_2 fixation by photochemical and enzymatic reduction is an inexpensive, attractive and green method for the synthesis of organic compounds from CO_2 as the starting material. Although several works have been done on CO_2 fixation, the quantum yields and selectivity of products based on the reduction of CO_2 are still low.[203-206] In artificial photocatalytic CO_2 reduction, reduction of CO_2 to CO is more favourable than to formic acid or other products. In principle, synthesis of formic acid by photocatalytic reduction of CO_2 is mainly done by using formate dehydrogenase (FDH) enzymes which catalyzes the reversible conversion of formic acid to CO_2. NADH- (nicotinamide adenine dinucleotide) dependent enzymes can be used to reduce the formed *N*,*N*′-alkyl-4,4′- or -2,2′-bipyridinium salt molecules as an artificial substrate instead of NADH or NAD^+. For example, FDH from *Saccharomyces cerevisiae* is a NADH-dependent enzyme and uses the various reduced forms of the bipyridinium salt molecules as a substrate for the conversion of CO_2 to formic acid.

Willner and co-workers reported the enzymatic formic acid synthesis from HCO_3^- with FDH and photoreduction of various 4,4′- or 2,2′-bipyridinium salts by a system containing $[Ru(bpy)_3]^{2+}$ (bpy = 2,2′-bipyridine) as a photosensitizer and mercaptoethanol (RSH) as an electron donor.[207-210] The efficiency of formic acid synthesis depends on the nature of the bipyridinium salts, and the quantum yield for formic acid from HCO_3^- is in the range of 0.5–1.6%. Schuchmann *et al.* reported the discovery of a bacterial hydrogen-dependent carbon dioxide reductase (HDCR) that directly uses H_2 for the interconversion of CO_2 to formate from the acetogenic bacterium *Acetobacterium woodii*.[211] They targeted this bacterium because it grows with H_2 + CO_2 under ambient conditions using an ancient pathway for CO_2 fixation and energy conservation. It lives under extreme energy limitation, and a directly uses H_2 for CO_2 reduction which would be beneficial for the cell.

Alissandratos *et al.* reported the biological conversion of CO_2 and H_2 into formate by utilising engineered whole-cell biocatalysts.[212] Escherichia coli JM109(DE3) cells transformed for overexpression of either native formate dehydrogenase (FDH), the FDH from Clostridium carboxidivorans, or genes from Pyrococcus furiosus and Methanobacterium thermoformicicum predicted to express FDH based on their similarity to known FDH genes were all able to produce levels of formate well above the background, when present with H_2 and CO_2.

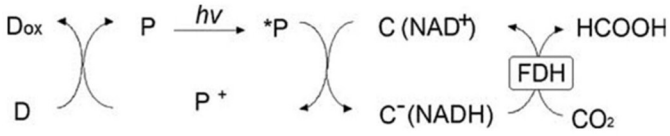

Fig. 12 Photochemical CO_2 reduction system that combines the photoreduction of NAD^+ as a electron relay by the photosensitization of dye molecules (P) and CO_2 reduction with FDH. Reprinted with permission from ref. 217. Copyright 2006 Elsevier.

Kodaka *et al.* reported direct synthesis of formic acid from CO_2 gas with the system consisting of triethanolamine (TEOA), $[Ru(bpy)_3]^{2+}$, various bipyridinium salts (1,1′-dialkyl-4,4′-bipyridinium salts or 1,1′-dialkyl-2,2′-bipyridinium salts) and FDH.[213] Effects of the structure and redox potentials of various bipyridinium salts have been investigated for the synthesis of formic acid from CO_2. After 7 h irradiation, the formation of formic acid in the concentration range of 0.2–0.95 mM was reached from a sample solution containing 0.5 M TEOA, 0.5 mM $[Ru(bpy)_3]^{2+}$, 3.0 mM bipyridinium salt, and 8 mg FDH. Best activity for formic acid synthesis from CO_2 was observed by using *N*,*N*′-trimethylene-2,2′-bipyridinium salt. Yield of

formic acid was depending on the redox potentials of the bipyridinium salts.

Amao and Miyatani synthesized formic acid from HCO_3^- with FDH and the photoreduction of *N*,*N*′-dimethyl-4,4′-bipyridinium (MV^{2+}).[214-216] They used water soluble zinc porphyrins (zinc tetrakis(4-methylpyridyl)porphyrin, ZnTMPyP) as a photosensitizer. When the sample solution containing 0.3 M TEOA, 9.0 μM $ZnTMPyP^{4+}$, 15 mM MV^{2+}, 20 units FDH and 1.0 mM $NaHCO_3$ was irradiated, 60 μm of formic acid (estimated yield 6%) was produced after 3 h of irradiation. In another report, they also introduced a system for synthesis of formic acid from CO_2 gas with FDH, MV^{2+}, NADPH as electron relay and Mg chlorophyll-a (MgChl-a) as visible light photosensitizer (Fig. 12).[217] After 4 h of irradiation, formation of 56 μM of formic acid was achieved from the sample solution containing NADPH (3.0 mM), MgChl-a (9.0 μM), MV^{2+} (0.1 mM), FDH (5 units), and CO_2 gas (saturated) at 303 K. Further, it has been observed that formic acid was not produced in the absence of any one of the components.

Sato and co-workers reported immobilization of a molecular CO_2 reduction catalyst onto a semiconductor surface for engineering hybrid photocatalytic materials.[218-222] The ruthenium catalysts were grafted onto different *p*-type semiconductors such as N-doped Ta_2O_5, Z-doped InP, *etc.* *via* covalent linkages or *via* a polymerization process. It was reported that the robustness of a hybrid system depends strongly on the choice of grafting linkages. The [Ru(dpbpy)(bpy)$(CO)_2$]/N–Ta_2O_5 (dpbpy = 4,4′-diphosphonate-2,2′-bipyridine, bpy = 2,2′-bipyridine) system with phosphate linker displayed a 5 times higher rate of CO_2 reduction to HCOOH (in acetonitrile solution using visible light) compared with the [Ru(dcbpy)(bpy)$(CO)_2$]/N–Ta_2O_5 (dcbpy: 4,4′-dicarboxy-2,2′-bipyridine, bpy = 2,2′-bipyridine) system with carbonate linker.[218,221] By using a Deronzier's-type ruthenium bipyridine-based polymeric film catalyst, a robust system adapted for working in aqueous solution was achieved.[221]

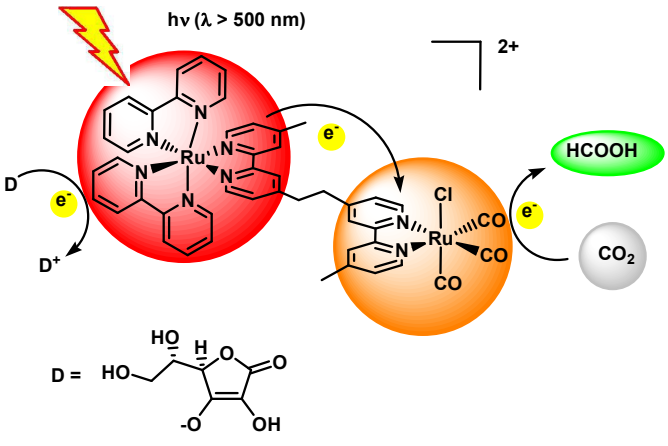

Fig. 13 Reaction pathways of the Photochemical Reduction of CO_2 to HCOOH by supramolecular Ru(II-Re(I) bimetallic complex with sodium ascorbate in an aqueous solution. Adopted with permission from ref. 223. Copyright 2015 Americal Chemical Society.

Recently, Ishitani and co-workers investigated photocatalytic reduction of CO_2 in an aqueous solution using supramolecular binuclear Ru(II)–Re(I) complex, of which Ru(II) photosensitizer and Re(I) catalyst units are connected with a bridging ligand (Fig. 13).[223] Sodium ascorbate used as an electron donor. Formic acid is the main product of photochemical reaction in aqueous solution (TON = 25, Selectivity = 83%) whereas CO is main product in DMF/TEOA.

4. Practical set up for formic acid based hydrogen storage

A sustainable cycle for energy storage based on formic acid and carbon dioxide can be designed as Fig. 14.[34]

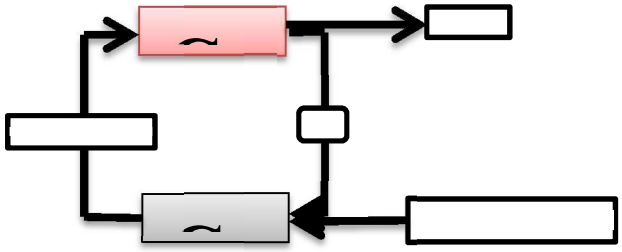

Fig. 14 A catalytic cycle for hydrogen storage in formic acid.

For energy storage, carbon dioxide is converted to formic acid or a formate derivative either electrochemically[224,225] or by catalytic hydrogenation.[32,156,226] The resulting material is a liquid at ambient conditions, either pure formic acid, an adduct containing formic acid, or an inorganic formate in aqueous solution, and can thus be handled, stored, and transported easily. On the other side of the cycle energy is released either in a direct formic acid fuel cell, or by selective on-demand decomposition in to carbon dioxide and hydrogen, which can be used directly in an appropriate hydrogen oxygen fuel cell.[227--232] If pure hydrogen is required the gases may also be separated using membrane techniques.[233] The hydrogen content of pure formic acid is 43 g/kg or 52 g/L, its release from formic acid is thermodynamically downhill by $\Delta G° = -32.8$ kJ/mol at room temperature.[156] As early as 1978, the electrochemical reduction of carbon dioxide to formic acid and its subsequent decomposition on Pd/C for energy storage have been proposed by Williams *et al.*[234] Later on, a system for solar energy conversion by reduction of aqueous carbonate was proposed by Halmann in 1983.[235] In 1986, a similar concept was described by Wiener *et al.* They proposed Pd/C catalyst to decompose aqueous formate solutions to obtain hydrogen.[236-238] However, both approaches have not led to any application. Two decades later, the research on the use of carbon dioxide for energy storage has been resumed in recent years.[6,34,61,239-242]

To identify the main technological obstacles on the way to an efficient use of FA as a hydrogen source and storage material, a hydrogen generator based on the decomposition of FA over a homogeneous Ru(II) catalyst was designed and built by Laurenczy and co-workers (Fig. 15).[6] The hydrogen generator successfully met the target power output of 1 kW_{el} or

roughly 30 L min^{-1} of H_2/CO_2 assuming 50% fuel cell efficiency. The system was designed around a 5 L reaction vessel with electrical surface heating elements, containing 11.8 g of $RuCl_3 \cdot 3H_2O$ (0.045 mol) and 51.2 g Na_3TPPTS (Na_3TPPTS sodium salt of *meta*-trisulfonated triphenylphosphine) (0.090 mol) catalyst in 1.5 L aqueous HCOONa solution (1 M). The free reactor volume (~3.5 L) is used as a buffer in case of rapid changes in the product flow rate set point as well as also serves for gas–liquid separation and effectively prevents foam or spray from reaching the product gas outlet.

Standard mass flow controller is utilized to control the product flow rate, while a controlled formic acid feed flow is utilized to maintain the reaction pressure. To minimize water vapour entrainment in the product gas, the system also comprises a product gas cooler with condensate separator/recycle. As the control concept does not comprise the measurement of pH or formic acid concentration in the catalyst solution, the reaction has to run at a large catalyst excess for reasons of process safety. This setup has been used safely for over one year without the need to exchange or replenish the catalyst solution.

In 2013, Beller *et al.* have been designed Ru(II)/dppe as the catalyst system for continuous hydrogen production from formic acid (Fig. 16).[243,244] The chemoselectivity is very high, resulting in very low CO contents of less than 10 ppm, which allows for its direct application for hydrogen generated in proton-exchange membrane (PEM) fuel cells. They presented the concept and insight of a setup for the continuous production of hydrogen from FA–amine adducts under mild conditions. This setup allows for a more secure system and a longer continuous hydrogen flow of up to 47 L/h. The continuous-

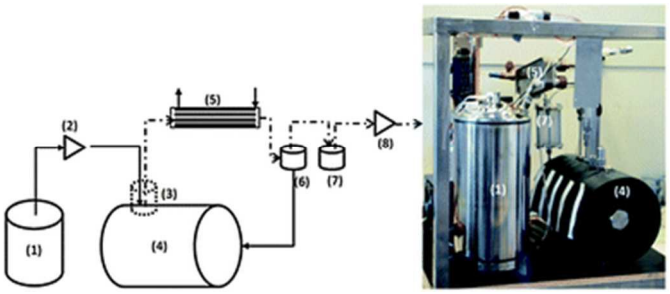

Fig. 15 A hydrogen generator designed and built in our laboratories for a power output of 1 kWel (30 L min−1 of H2/CO2) (1) Formic acid tank; (2) pump; (3) tube in tube heat exchanger; (4) reactor; (5) heat exchanger; (6 and 7) condensate separators; (8) mass flow controller. Adopted with permission from ref. 6. Copyright 2012 Royal Society of Chemistry.

-setup consists of four main parts (Fig. 16): the high pressure reactor, the FA dosage system, the gas cleaning unit, and the quantification and analysis part for the resulting gas mixture. Central parts to control the dosage of FA are the pump and the liquid flow meter. The reactor, a stainless-steel autoclave, is connected to a condenser, a gas filter, and an active carbon column. These will remove any traces of discharged liquids or vapors. All components are commercially available. To produce hydrogen on demand, a certain amount of FA is dosed into the reactor containing the catalyst and the amine, and immediately, it is converted to hydrogen and carbon dioxide, in the same way that gasoline is consumed in an Otto engine. This allows for the use of the full hydrogen density of the FA of 4.4 wt% (not including surrounding system) because only the acid

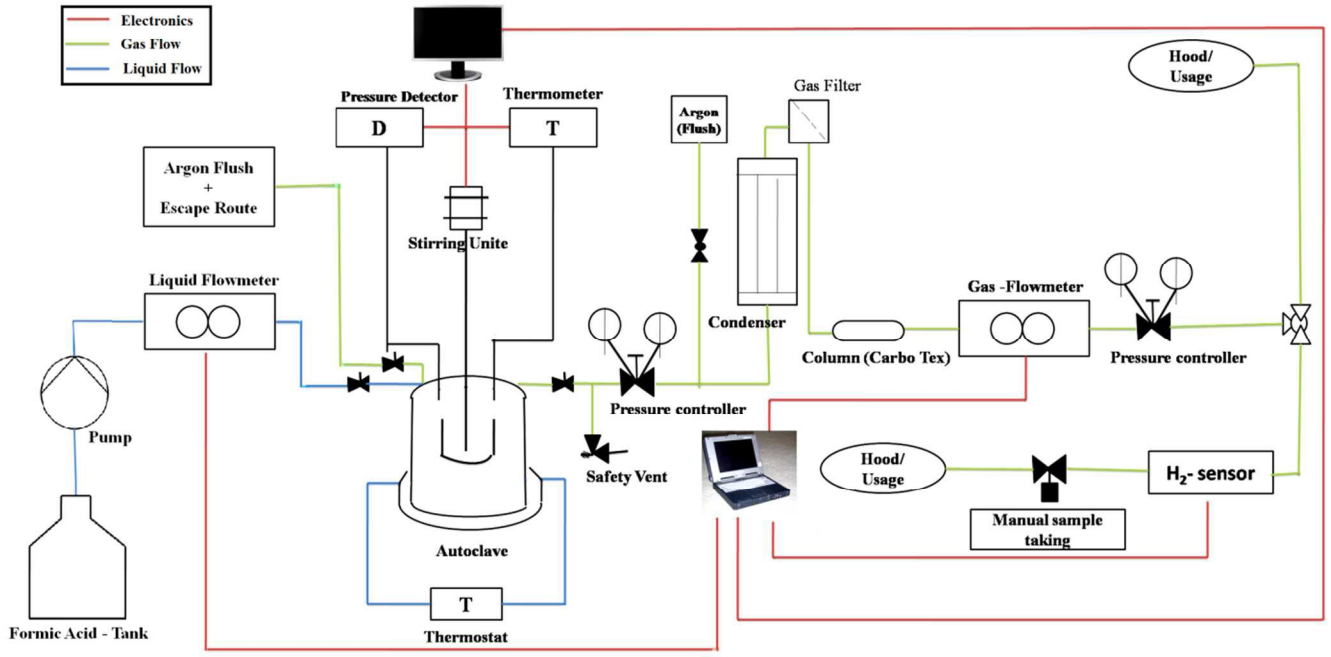

Fig. 16 Schematic representation of the setup used for continuous hydrogen production. Reprinted with permission from ref. 243. Copyright 2013 Wiley-VCH.

has to be stored in a tank.

Beller *et al.* also developed a reversible "hydrogen-battery" which allowed reversible fast hydrogen loading (even at RT) and unprecedented unloading (TON for H_2 liberation of 800 000).[244] For this purpose they used defined $[RuH_2(dppm)_2]$ complex instead of the *in situ* catalyst system. With this catalyst hydrogenation of carbon dioxide and hydrogen release from the resulting formic acid were possible up to eight consecutive at room temperature.

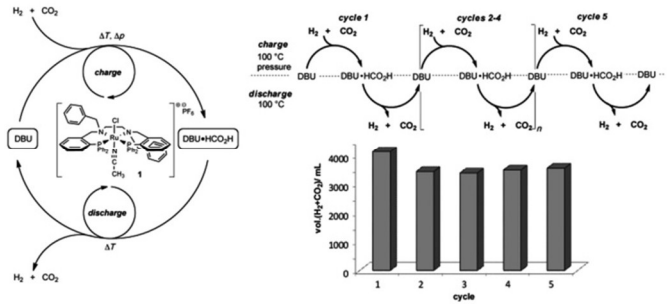

Fig. 17 Schematic for charging and discharging process developed by Plietker *et al.* and Charging and discharging cycles of the H_2 battery. Reprinted with permission from ref. 245. Copyright 2013 Wiley-VCH.

Group of Plietker reported a rechargeable H_2 battery based on the principle of the Ru-catalyzed hydrogenation of CO_2 to formic acid (charging process) and the Ru-catalyzed decomposition of formic acid to CO_2 and H_2 (discharging process).[245] Both processes are driven by the same catalyst at elevated temperature either under pressure (charging process) or pressure-free conditions (discharging process). Up to five charging–discharging cycles were performed without decrease of storage capacity. The resulting CO_2/H_2 mixture is free of CO and can be employed directly in fuel-cell technology (Fig. 17).

Some rechargeable hydrogen batteries were developed based on selective hydrogenation of bicarbonates and the selective dehydrogenation of formates, instead of hydrogenation of CO_2 and dehydrogenation of formic acid. Beller and co-workers have presented a ruthenium-based catalyst system ([{$RuCl_2$(benzene)}$_2$]/dppm (Ru/P=1:6)) for the selective hydrogenation of bicarbonates and the selective dehydrogenation of formats (Fig. 18).[246] It was demonstrated that the two reactions can be coupled leading to a reversible hydrogen-storage system. Hydrogenation of $NaHCO_3$ to sodium formate was performed in 96 % yield at 343 K in water/THF without additional CO_2. Dehydrogenation of sodium formate was achieved with high conversion (>90 %) under ambient temperature (303 K). In contrast to the dehydrogenation of formic acid/amine adducts this process is amine-free.

Fig. 18 Reversible hydrogen storage with a bicarbonate/formate system: Catalytic

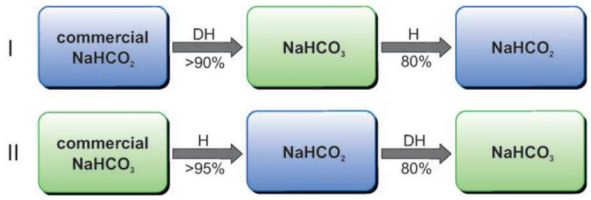

hydrogenation of bicarbonate and hydrogen release from formate with the same Ru/dppm in situ catalyst. Reaction conditions: dehydrogenation (DH): 40 mL DMF, 10 mL H_2O, 303 K, 24–48 h; hydrogenation (H): 20 mL H_2O, 10 mL THF, 80 bar H_2, 24 h; sequence I: 71 µmol [{$RuCl_2$(benzene)}$_2$], 0.43 mmol dppm, 39.6 mmol $NaHCO_2$; sequence II: 10.4 µmol [{$RuCl_2$(benzene)}$_2$], 41.6 µmol dppm, 23.8 mmol $NaHCO_3$. Reprinted with permission from ref. 246. Copyright 2013 Wiley-VCH.

Cao and co-workers developed the first heterogeneous catalytic system (1 wt % Pd/r-GO, Pd NPs supported on reduced graphene (rGO)) for the efficient reversible dehydrogenation of aqueous formates to bicarbonates.[247] The r-GO nanosheets are a distinct and powerful support allowing for the generation of highly strained Pd NPs that enable facile and repetitive formate/bicarbonate interconversion under mild aqueous conditions. By controlling the temperature and the hydrogen pressure, the reversible catalytic transformations can be repeated nearly quantitatively six times with almost no loss of efficiency. This could lead to the construction of a simple, truly rechargeable HCOOK/$KHCO_3$-based hydrogen storage device.

Ammonium bicarbonate/formate redox equilibrium system has also been demonstrated for reversible hydrogen storage and evolution using the same Pd/AC nanocatalyst by Lin and co-workers.[248] Reaction temperature and H_2 pressure are key factors in controlling the hydrogen storage–evolution equilibrium in this system. Up to 96 % yield of ammonium formate was achieved when the hydrogenation reaction was carried out at room temperature at an initial hydrogen pressure of 2.75 MPa, whereas nearly 100 % hydrogen yield was obtained from the dehydrogenation of ammonium formate at 353 K at an initial nitrogen pressure of 0.1 MPa. Compared to the homogeneous catalytic system, this heterogeneous system has the following advantages: no organic solvents or inorganic additives are needed; high volumetric energy density of hydrogen (stored in concentrated ammonium formate aqueous solutions) is achieved; the solid salts or their aqueous solutions can be easily transported and distributed; and the Pd/AC catalyst is stable, being more easily recycled and handled than homogeneous catalysts.

Further work on the design and test of the hydrogen battery device based on reversible catalytic system for formic acid dehydrogenation/hydrogenation of CO_2 as well as dehydrogenation of formate/hydrogenation of bicarbonates are still under progress.

5. Conclusions and Perspectives

In this review, we have focused on the application of formic acid as a renewable hydrogen energy source for future. In addition, we have tried to focus on formic acid production from various processes and at the same time possibility of its regeneration from green house gas CO_2 has also been explored. We have attempted to present an up-to-date overview of this rapidly growing field of research. This subject area is very active and many papers are published every year (even during the preparation of this review) by chemists, physical and materials scientists. Therefore, it is difficult to take into account all the contributions to this field in a limited number of pages. We apologize if some significant contributions have been left out.

In the first part, we have summarized recent development in formic acid decomposition reactions catalysed either by homogeneous as well as heterogeneous catalysts in the presence and absence of base and other additives. For improvement of catalytic performance, it is required to facilitate the activation of the C–H bond of formate anion which is anticipated to be the rate-limiting step. Majority of homogeneous catalytic system are based on Ru/Rh/Ir/Fe complexes where as Pd is the main constituent of heterogeneous catalyst.

Extensive works on homogeneous catalytic decomposition of FA have been done by Beller and Leuranczy *et al.* Thanks to the people working in the field to prepare low-cost and efficient catalyst for hydrogen generation from formic acid. For homogeneous catalysts, β-hydride elimination is the rate determining step of FA dehydrogenation. Thus, lowering the activation energy of β-hydride elimination is a key of success for enhancing activity and selectivity of FA dehydrogenation. Scientists achieved this goal by modifying different parameters of the catalyst systems e.g. metal centre, design of ligands, reaction temperature, solvent medium and additives (phosphine/base/salts) etc. One of the recent approaches as suggested by Chauvier *et al.*, is to use a Lewis acid capable of converting formate anion to CO_2, with a low activation energy and negligible exergonicity.[73]

As obvious for most of the heterogeneous catalytic processes, activity/selectivity of heterogeneous catalytic FA dehydrogenation process also depends upon sizes, morphologies, distributions, and surface states of NPs, capping agents, catalyst support, for bi-/tri-metallic NPs counter elements. Generally, the smaller size particles have better catalytic activity because of large surface area but they are easy to aggregate due to their high surface energy and so induce low activity. Hence, suitable capping agent or support is required for dispersion of NPs to avoid the aggregation without severe deactivation of surface of NPs by strong affiliation of capping agent or support. In FA dehydrogenation process, unsupported Pd catalysts are inactive due to aggregation of NPs as well as poisoning of surface by CO formed upon FA decomposition. Good activity with high selectivity for FA dehydrogenation was accomplished by immobilization of Pd NPs on/in carbon/graphene/silica/zirconia/ceria supports etc. These supports not only facilitate dispersion of metal NPs but also catalytic CO oxidation at metal-support interface, thus, prevent deactivation of catalyst by CO poisoning.

Similarly, in bimetallic NPs, second component such as Au or Ag helps to diminish CO production by FA decomposition. As a result, reaction proceeds *via* FA dehydrogenation with enhanced activity and selectivity. To further understand/explain the mechanism involved in formic acid decomposition on surface, density functional theoretical approaches have also been adopted.

In second part, we tried to cover various methods to prepare formic acid with special emphasis on biomass conversion to formic acid as well as CO_2 hydrogenation by different methods. Wasserscheid and co-workers developed a method to get formic acid and CO_2 selectively by different types of biomasses either water soluble or insoluble. By varying the reaction condition such as pH, temperature or biomass substrate, they were successful in getting formic acid up to 60% selectivity. We have also discussed CO_2 reduction or hydrogenation to formic acid in detail. CO_2 hydrogenation to FA is depending on initial pressure of the reactant (H_2 and CO_2), solvent etc. Basic condition favours formation of FA in high yield owing to neutralization of acid product. Presence of basic sites, on supported/heterogeneous catalysts, induces initial interaction with CO_2 for the synthesis of FA also. Better catalytic performance could be achieved by tuning such interactions.

Some catalyst systems are active for both dehydrogenation of formic acid as well as hydrogenation of CO_2 by varying the reaction condition only, as a result providing an opportunity for the charge/discharge of hydrogen fuel cells similar to other rechargeable batteries. Beller and others developed few rechargeable hydrogen-batteries based on these reversible catalyst systems, as summarized in third part.

Besides the several advantages, formic acid based hydrogen storage system has only 4.4 wt% hydrogen content which gets further decreased by addition of amine as well as solvent to around 1%. To meet practical applications, further work is needed for the development of low-cost, more efficient, reversible catalyst systems. Moreover, development of photocatalytic systems for both the processes (fixation and the evolution of hydrogen to/from formic acid), which employs sustainable/renewable energy resources, is highly desirable.

Acknowledgements

The authors thank the reviewers for their valuable suggestions. AK thanks DST for the financial support. AKS and SBS acknowledge the UGC for DSK Postdoctoral Fellowship. The authors are thankful to who have worked in this area; their names can be found in the references section. AKS is grateful to Prof. Q. Xu, AIST, Ikeda, Osaka for his generous support and guidance during his postdoc in Japan.

Notes and references

[a] Department of Inorganic and Physical Chemistry, Indian Institute of Science, Bangalore-560012, India Email: ashish.bhuchem@gmail.com Mob. No.: +91 9450209554

[b] Department of Solid State structural Characterization Unit, Indian Institute of Science, Bangalore-560012, India Email: sbs.bhu@gmail.com Mob. No.: +91 9453269249
[c]Department of Chemistry, University of Lucknow, Lucknow 226007, India Email: abhinavmarshal@gmail.com Mob. No.: +91 9451891030

References

1 L. Schlapbach and A. Züttel, *Nature*, 2001, **414**, 353–358.
2 J. Graetz, *Chem. Soc. Rev.*, 2009, **38**, 73–82.
3 U. B. Demirci and P. Miele, *Energy Environ. Sci.*, 2011, **4**, 3334–3341.
4 B. Loges, A. Boddien, F. Gartner, H. Junge and M. Beller, *Top. Catal.*, 2010, **53**, 902–914.
5 P. Makowski, A. Thomas, P. Kuhn and F. Goettman, *Energy Environ. Sci.*, 2009, **2**, 480–490.
6 M. Grasemann and G. Laurenczy, *Energy Environ. Sci.*, 2012, **5**, 8171–8181.
7 F. Joó, *ChemSusChem*, 2008, **1**, 805–808.
8 A. K. Singh and Q. Xu, *Chemcatchem*, 2013, **5**, 652–676.
9 M. Yadav and Q. Xu, *Energy Environ. Sci.*, 2012, **5**, 9698–9725.
10 E. Fujita, J. T. Muckerman and Y. Himeda, *Biochim. Biophys. Acta*, 2013, **1827**, 1031–1038.
11 S. Enthaler, J. von Langermann and T. Schmidt, *Energy Environ. Sci.*, 2010, **3**, 1207–1217.
12 S. L. Li and Q. Xu, *Energy Environ. Sci.*, 2013, **6**, 1656−1683.
13 A. W. C. van den Berg and C. O. Areán, *Chem. Commun.*, 2008, 668−681
14 F. Amaseder and G. Krainz, Liquid hydrogen storage systems developed and manufactured for the first time for customer cars. In: SAE paper 2006-01-0432; 2006.
15 S. M. Aceves, F. Espinosa-Loza, E. Ledesma-Orozco, T. O. Ross, A. H. Weisberg, T.C. Brunner and O. Kircher, *Int. J. Hyd. Energy*, 2010, **35**, 1219–1226.
16 B. Sakintuna and Y. Yürüm, *Ind. Eng. Chem. Res.*, 2005, **44**, 2893–2902
17 A. C. Dillon, K. M. Jones, T. A. Bekkedahl, C. H. Kiang, D. S. Bethune and M. J. Heben, *Nature*, 1997, **386**, 377–379.
18 A. D. Lueking, R. T. Yang, N. M. Rodríguez and R. T. K. Baker, *Langmuir*, 2004, **20**, 714–721.
19 W. Chaikittisilp, K. Ariga and Y. Yamauchi, *J. Mater. Chem. A*, 2013, **1**, 14−19.
20 J. Weitkamp, M. Fritz and S. Ernst, *Int. J. Hydrogen Energy*, 1995, **20**, 967–970.
21 A. Zuttle, *Mater. Today*, 2003, **6**, 24–33.
22 H. Lee, J. W. Lee, D. Y. Kim, J. Park, Y. Seo, H. Zeng, I. L. Moudrakovskl, C. I. Ratcliffe and J. A. Ripmeester, *Nature*, 2005, **434**, 743−746.
23 Y. H. Hu and E. Ruckenstein, *Angew. Chem., Int. Ed.*, 2006, **45**, 2011−2013.
24 J. L. C. Roswell and O. M. Yaghi, *Angew. Chem., Int. Ed.*, 2005, **44**, 4670–4679.
25 M. P. Suh, H. J. Park, T. K. Prasad and D.-W. Lim, *Chem. Rev.*, 2012, **112**, 782−835.
26 M. Dinca and J. R. Long, *J. Am. Chem. Soc.*, 2005, **127**, 9376−9377.
27 X. Lin, J. Jia, X. Zhao, K. M. Thomas, A. J. Blake, G. S. Walker, N. R. Champness, P. Hubberstey and M. Schröder, *Angew. Chem., Int. Ed.*, 2006, **45**, 7358−7364.
28 D. R. Hoffman, "Ant venoms" *Curr. Opin. Allergy. Clin. Immunol.*, 2010, **10**, 342–346.
29 M. Carmo, D. L. Fritz, J. Mergel and D. Stolten, *Int. J. Hydrogen Energy*, 2013, **38**, 4901–4934.
30 M. E. Boot-Handford, J. C. Abanades, E. J. Anthony, M. J. Blunt, S. Brandani, N. M. Dowell, J. R. Fernández, M.-C. Ferrari, R. Gross, J. P. Hallett, R. S. Haszeldine, P. Heptonstall, A. Lyngfelt, Z. Makuch, E. Mangano, R. T. J. Porter, M. Pourkashanian, G. T. Rochelle, N. Shah, J. G. Yao and P. S. Fennell, *Energy Environ. Sci.*, 2014, **7**, 130–189.
31 Y. Yasaka, H. Yoshida, C. Wakai, N. Matubayasi and M. Nakahara, *J. Phys. Chem. A*, 2006, **110**, 11082–11090.
32 P. G. Jessop, F. Joó and C.-C. Tai, *Coord. Chem. Rev.*, 2004, **248**, 2425–2442.
33 J. A. Turner, *Science*, 2004, **305**, 972–974.
34 T. C. Johnson, D. J. Morris and M. Wills, *Chem. Soc. Rev.*, 2010, **39**, 81–88.
35 Office of Energy Efficiency and Renewable Energy; The Freedom CAR and Fuel Partnership, Targets For Onboard Hydrogen Storage Systems For Light-duty Vehicles, September 2009, http://www1.eere.energy.gov.
36 J. Yang, A. Sudik, C. Wolverton and D. J. Siegel, *Chem. Soc. Rev.*, 2010, **39**, 656–675.
37 A. F. Dalebrook, W. Gan, M. Grasemann, S. Moret and G. Laurenczy, *Chem. Commun.*, 2013, **49**, 8735–8751.
38 A. Behr and K. Nowakowski, *Advances in Inorganic Chemistry*, 2014, **66**, 223–258.
39 D. Teichmann, W. Arlt, P. Wasserscheid and R. Freymann, *Energy Environ. Sci.*, 2011, **4**, 2767–2773.
40 D. Teichmann, W. Arlt and P. Wasserscheid, *Int. J. Hydrogen Energy*, 2012, **37**, 18118–18132.
41 M. Nielsen, E. Alberico, W. Baumann, H.-J. Drexler, H. Junge, S. Gladiali and M. Beller, *Nature*, 2013, **495**, 85–89.
42 A. Monney, E. Barsch, P. Sponholz , H. Junge, R. Ludwig and M. Beller, *Chem. Commun.*, 2014, **50**, 707–709.
43 X. Yu, P. G. Pickup, *J. Power Sources*, 2008, **182**, 124–132.
44 R. S. Coffey, *Chem. Commun.*, 1967, 923–924.
45 S. H. Strauss, K. H. Whitmire and D. F. Shriver, *J. Organomet. Chem.*, 1979, **174**, C59–C62.
46 R. S. Paonessa and W. C. Trogler, *J. Am. Chem. Soc.*, 1982, **104**, 3529–3530.
47 R. B. King and N. K. Bhattacharyya, *Inorg. Chim. Acta*, 1995, **237**, 65–69.
48 J. H. Shin, D. G. Churchill and G. Parkin, *J. Organomet. Chem.*, 2002, **642**, 9–15.
49 Y. Gao, J. Kuncheria, G. P. A. Yap and R. J. Puddephatt, *Chem. Commun.*, 1998, 2365–2366.
50 Y. Gao, J. K. Kuncheria, H. A. Jenkins, R. J. Puddephatt and G. P. A. Yap, *J. Chem. Soc., Dalton Trans.*, 2000, 3212–3217.
51 B. Loges, A. Boddien, H. Junge and M. Beller, *Angew. Chem., Int. Ed.*, 2008, **47**, 3962–3965.
52 A. Boddien, B. Loges, H. Junge and M. Beller, *ChemSusChem*, 2008, **1**, 751–758.

53 H. Junge, A. Boddien, F. Capitta, B. Loges, J. R. Noyes, S. Gladiali and M. Beller, *Tetrahedron Lett.*, 2009, **50**, 1603–1606.
54 X. Li, X. Ma, F. Shi and Y. Deng, *ChemSusChem*, 2010, **3**, 71–74.
55 X. Li, F. Shi, X. Ma, L. Lu and Y. Deng, *J. Fuel Chem. Technol.*, 2010, **38**, 544–553.
56 M. E. M. Berger, D. Assenbaum, N. Taccardi, E. Spiecker and P. Wasserscheid, *Green Chem.*, 2011, **13**, 1411–1415.
57 C. Fellay, P. J. Dyson and G. Laurenczy, *Angew. Chem., Int. Ed.*, 2008, **47**, 3966–3968.
58 C. Fellay, N. Yan, P. J. Dyson and G. Laurenczy, *Chem. Eur. J.*, 2009, **15**, 3752–3760.
59 W. Gan, P. J. Dyson and G. Laurenczy, *React. Kinet. Catal. Lett.*, 2009, **98**, 205–213.
60 D. J. Morris, G. J. Clarkson and M. Wills, *Organometallics*, 2009, **28**, 4133–4140.
61 A. Majewski, D. J. Morris, K. Kendall and M. Wills, *ChemSusChem*, 2010, **3**, 431–434.
62 I. Mellone, M. Peruzzini, L. Rosi, D. Mellmann, H. Junge, M. Beller, and L. Gonsalvi, *Dalton Trans.*, 2013, **42**, 2495–2501.
63 G. Manca, I. Mellone, F. Bertini, M. Peruzzini, L. Rosi, D. Mellmann, H. Junge, M. Beller, A. Ienco and L. Gonsalvi, *Organometallics*, 2013, **32**, 7053–7064.
64 S. Enthaler, H. Junge, A. Fischer, A. Kammer, S. Krackl and J. D. Epping, *Polym. Chem.*, 2013, **4**, 2741–2746.
65 S. Fukuzumi, T. Kobayashi and T. Suenobu, *ChemSusChem*, 2008, **1**, 827–834.
66 Y. Himeda, *Green Chem.*, 2009, **11**, 2018–2022.
67 S. Fukuzumi, T. Kobayashi and T. Suenobu, *J. Am. Chem. Soc.*, 2010, **132**, 1496–1497.
68 S. Oldenhof, B. de Bruin, M. Lutz, M. A. Siegler, F. W. Patureau, J. I. van der Vlugt and J. N. H. Reek, *Chem. Eur. J.*, 2013, **19**, 11507–11511.
69 A. Boddien, B. Loges, F. Gärtner, C. Torborg, K. Fumino, H. Junge, R. Ludwig and M. Beller, *J. Am. Chem. Soc.*, 2010, **132**, 8924–8934.
70 A. Boddien, D. Mellmann, F. Gärtner, R. Jackstell, H. Junge, P. J. Dyson, G. Laurenczy, R. Ludwig and M. Beller, *Science*, 2011, **333**, 1733–1734.
71 D. Mellmann, E. Barsch, M. Bauer, K. Grabow, A. Boddien, A. Kammer, P. Sponholz, U. Bentrup, R. Jackstell, H. Junge, G. Laurenczy, R. Ludwig and M. Beller, *Chem. Eur. J.*, 2014, **20**, 13589–13602.
72 T. Zell, B. Butschke, Y. Ben-David and D. Milstein, *Chem. Eur. J.*, 2013, **19**, 8068–8072.
73 E. A. Bielinski, P. O. Lagaditis, Y. Zhang, B. Q. Mercado, C. Würtele, W. H. Bernskoetter, N. Hazari and S. Schneider, *J. Am. Chem. Soc.*, 2014, **136**, 10234−10237.
74 T. W. Myers and L. A. Berben, *Chem. Sci.*, 2014, **5**, 2771−2777.
75 K. Hirota, K. Kuwata and Y. Nakai, *Bull. Chem. Soc. Jpn.*, 1958, **31**, 861–864.
76 D. H. S. Ying and R. J. Madix, *J. Catal.*, 1980, **61**, 48–56.
77 Y. K. Sun, J. J. Vajo, C. Y. Chan and W. H. Weinberg, *J. Vac. Sci. Technol. A*, 1988, **6**, 854–855.
78 X. D. Peng and M. A. Barteau, *Catal. Lett.*, 1991, **7**, 395–402.
79 N. Aas, Y. Li and M. Bowker, *J. Phys. Condens. Matter.*, 1991, **3**, S281–S286.
80 P. A. Dilara and J. M. Vohs, *J. Phys. Chem.*, 1993, **97**, 12919–12923.
81 V. A. Gercher and D. F. Cox, *Surf. Sci.*, 1994, **312**, 106–114.
82 J. Stubenrauch, E. Brosha and J. M. Vohs, *Catal. Today*, 1996, **28**, 431–444.
83 R. Larsson, M. H. Jamroz and M. A. Borowiak, *J. Mol. Catal. A*, 1998, **129**, 41–51.
84 A. Bandara, J. Kubota and A. Wada, *J. Phys. Chem. B*, 1997, **101**, 361–368.
85 J. Rasko, T. Kecskes and J. Kiss, *J. Catal.*, 2004, **224**, 261–268.
86 T. Shido and Y. Iwasawa, *J. Catal.*, 1993, **141**, 71–81.
87 G. Jacobs, P. M. Patterson, U. M. Graham, A. C. Crawford and B. H. Davis, *Int. J. Hydrogen Energy*, 2005, **30**, 1265–1276.
88 G. Jacobs, P. M. Patterson, U. M. Graham, A. C. Crawford, A. Dozier and B. H. Davis, *J. Catal.*, 2005, **235**, 79–91.
89 M. Ojeda and E. Iglesia, *Angew. Chem. Int. Ed.*, 2009, **48**, 4800–4803.
90 D. A. Bulusheva, S. Beloshapkin and J. R. H. Ross, *Catal. Today*, 2010, **154**, 7–12.
91 F. Solymosi, Á. Koós, N. Liliom and I. Ugrai, *J. Catal.*, 2011, **279**, 213–219.
92 G. Halasi, G. Schubert and F. Solymosi, *Catal. Lett.*, 2011, **142**, 218–223.
93 D. A. Bulushev, L. Jia, S. Beloshapkin and J. R. H. Ross, *Chem. Commun.*, 2012, **48**, 4184–4186.
94 X. Zhou, Y. Huang, W. Xing, C. Liu, J. Liao and T. Lu, *Chem. Commun.*, 2008, 3540–3542.
95 Y. Huang, X. Zhou, M. Yin, C. Liu and W. Xing, *Chem. Mater.,* 2010, **22**, 5122–5128.
96 G. Glaspell, L. Fuoco and M. S. El-Shall, *J. Phys. Chem. B*, 2005, **109**, 17350–17355.
97 W.-J. Shen and Y. Matsumura, *J. Mol. Catal. A*, 2000, **153**, 165–168.
98 X. Zhou, Y. Huang, C. Liu, J. Liao, T. Lu and W. Xing, *ChemSusChem*, 2010, **3**, 1379–1382.
99 S. W. Ting, S. Cheng, K. Y. Tsang, N. van der Laak and K. Y. Chan, *Chem. Commun.*, 2009, 7333–7335.
100 K. Tedsree, T. Li, S. Jones, C. W. A. Chan, K. M. K. Yu, P. A. J. Bagot, E. A. Marquis, G. D. W. Smith and S. C. E. Tsang, *Nat. Nanotechnol.*, 2011, **6**, 302–307.
101 K. Tedsree, C. W. A. Chan, S. Jones, Q. Cuan, W. K. Li, X. Q. Gong and S. C. E. Tsang, *Science*, 2011, **332**, 224–228.
102 Z.-L. Wang, J.-M. Yan, H.-L. Wang, Y. Ping and Q. Jiang, *Sci. Rep.*, 2012, **2**, 598.
103 Z.-L. Wang, J.-M. Yan, H.-L. Wang, Y. Ping and Q. Jiang, *J. Mater. Chem. A*, 2013, **1**, 12721–12725.
104 Y. Ping, J.-M. Yan, Z.-L. Wang, H.-L. Wang and Q. Jiang, *J. Mater. Chem. A*, 2013, **1**, 12188–12191.
105 Z.-L. Wang, J.-M. Yan, Y. Ping, H.-L. Wang, W.-T. Zheng and Q. Jiang, *Angew. Chem. Int. Ed.*, 2013, **52**, 4406–4409.
106 Z.-L. Wang, Y. Ping, J.-M. Yan, H.-L. Wang and Q. Jiang, *Int. J. Hydrogen Energy*, 2014, **39**, 4850–4856.
107 Z.-L. Wang, H.-L. Wang, J.-M. Yan, Y. Ping, Song-Il O, S.-J. Li and Q. Jiang, *Chem. Commun.*, 2014, **50**, 2732–2734.
108 M. Yadav, A. K. Singh, N. Tsumori and Q. Xu, *J. Mater. Chem.*, 2012, **22**, 19146–19150.
109 Y.-Y. Cai, X.-H. Li, Y.-N. Zhang, X. Wei, K.-X. Wang and J.-S. Chen, *Angew. Chem. Int. Ed.*, 2013, **52**, 11822–11825.

110 K. Mori, M. Dojo and H. Yamashita, *ACS Catal.*, 2013, **3**, 1114–1119.
111 Q.-L. Zhu, N. Tsumori and Q. Xu, *Chem. Sci.*, 2014, **5**, 195–199.
112 X. Gu, Z.-H. Lu, H.-L. Jiang, T. Akita and Q. Xu, *J. Am. Chem. Soc.*, 2011, **133**, 11822–11825.
113 H. Dai, N. Cao, L. Yang, J. Su, W. Luo and G. Cheng, *J. Mater. Chem. A*, 2014, **2**, 11060–11064.
114 M. Martis, K. Mori, K. Fujiwara, W.-S. Ahn and H. Yamashita, *J. Phys. Chem. C*, 2013, **117**, 22805–22810.
115 Y.-L. Qin, J. Wang, F.-Z. Meng, L.-M. Wang and X.-B. Zhang, *Chem. Commun.*, 2013, **49**, 10028–10030.
116 M. Yadav, T. Akita, N. Tsumori and Q. Xu, *J. Mater. Chem.*, 2012, **22**, 12582–12586.
117 Q.-Y. Bi, X.-L. Du, Y.-M. Liu, Y. Cao, H.-Y. He and K.-N. Fan, *J. Am. Chem. Soc.*, 2012, **134**, 8926–8933.
118 L. Jia, D. A. Bulushev, O. Y. Podyacheva, A. I. Boronin, L. S. Kibis, E. Y. Gerasimov, S. Beloshapkin, I. A. Seryak, Z. R. Ismagilov and J. R. H. Ross, *J. Catal.*, 2013, **307**, 94–102.
119 M. Yurderi, A. Bulut, M. Zahmakiran and M. Kaya, *Appl. Catal. B*, 2014, **160–161**, 514–524.
120 K. Jiang, K. Xu, S.-Z. Zou and W.-B. Cai, *J. Am. Chem. Soc.*, 2014, **136**, 4861–4864.
121 J. H. Lee, J. Ryu, J. Y. Kim, S.-W. Nam, J. H. Han, T.-H. Lim, S. Gautam, K. H. Chae and C. W. Yoon, *J. Mater. Chem. A*, 2014, **2**, 9490–9495.
122 Q. Luo, G. Feng, M. Beller and H. Jiao, *J. Phys. Chem. C*, 2012, **116**, 4149–4156.
123 Q. Luo, T. Wang, M. Beller and H. Jiao, *J. Mole. Catal. A*, 2013, **379**, 169–177
124 Q. Luo, T. Wang, M. Beller and H. Jiao, *J. Power Sources*, 2014, **246**, 548–555.
125 Q. Luo, M. Beller and H. Jiao, *J. Theor. Comput. Chem.*, 2013, **12**, 1330001.
126 http://en.wikipedia.org/wiki/Formic_acid.
127 New study confirms that nature is responsible for 90% of the Earth's atmospheric acidity – wattsupwiththat.com.
128 W. Reutemann and H. Kieczka "Formic Acid" in Ullmann's Encyclopedia of Industrial Chemistry 2002, Wiley-VCH, Weinheim.
129 M. Aresta, A. Dibenedetto and A. Angelini, *Chem. Rev.*, 2014, **114**, 1709–1742.
130 R. Miyatani and Y. Amao, *Biotechnol. Lett.*, 2002, **24**, 1931–1934.
131 R. Miyatani and Y. Amao, *J. Mol. Catal. B.*, 2004, **27**, 121–125.
132 J. Song, H. Fan, J. Ma and B. Han, *Green Chem.*, 2013, **15**, 2619–2635.
133 N. Taccardi, D. Assenbaum, M. E. M. Berger, A. Bosmann, F. Enzenberger, R. Wolfel, S. Neuendorf, V. Goeke, N. Schodel, H. J. Maass, H. Kistenmacher and P. Wasserscheid, *Green Chem.*, 2010, **12**, 1150–1156.
134 D. Yu, M. Aihara and J. Antal, *Energy Fuels*, 1993, **7**, 574–577.
135 G. D. Mcginnis, S. E. Prince, C. J. Biermann and J. T. Lowrimore, *Carbohydr. Res.*, 1984, **128**, 51–60.
136 G. D. Mcginnis, W. W. Wilson and C. E. Mullen, *Ind. Eng. Chem. Prod. Res. Dev.*, 1983, **22**, 352–357.
137 F. M. Jin, J. Yun, G. M. Li, A. Kishita, K. Tohji and H. J. Enomoto, *Green Chem.*, 2008, **10**, 612–615.
138 R. Wölfel, N. Taccardi, A. Bösmann and P. Wasserscheid, *Green Chem.*, 2011, **13**, 2759–2763.
139 J. Albert, R. Wölfel, A. Bösmann and P. Wasserscheid, *Energy Environ. Sci.*, 2012, **5**, 7956–7962
140 J. Albert, D. Lüders, A. Bösmann, D. M. Guldi and P. Wasserscheid, *Green Chem.*, 2014, **16**, 226–237.
141 J. Li, D.-J. Ding, L. Deng, Q.-X. Guo and Y. Fu, *ChemSusChem*, 2012, **5**, 1313–1318.
142 J. Zhang, M. Sun, X. Liu and Y. Han, *Catal. Today*, 2014, **233**, 77–82.
143 J. Xu, H. Zhang, Y. Zhao, Z. Yang, B. Yu, H. Xu and Z. Liu, *Green Chem.*, 2014, **16**, 4931–4935
144 W. Wang, M. Niu, Y. Hou, W. Wu, Z. Liu, Q. Liu, S. Ren and K. N. Marsh, *Green Chem.*, 2014, **16**, 2614–2618.
145 Z. Tang, W. Deng, Y. Wang, E. Zhu, X. Wan, Q. Zhang and Y. Wang, *ChemSusChem*, 2014, **7**, 1557–1567.
146 P. Gao, G. Li, F. Yang, X.-N. Lv, H. Fan, L. Meng and X.-Q. Yu, *Ind. Crops Prod.*, 2013, **48**, 61–67.
147 F. Jin, J. Yun, G. Li, A. Kishita, K. Tohji and H. Enomoto, *Green Chem.*, 2008, **10**, 612–615.
148 H. Choudhary, S. Nishimura and K. Ebitani, *Appl. Catal. B*, 2015, **162**, 1–10.
149 M. Cokoja, C. Bruckmeier, B. Rieger, W. A. Herrmann and F. E. Kühn, *Angew. Chem. Int. Ed.*, 2011, **50**, 8510–8537.
150 G. A. Olah, *Angew. Chem. Int. Ed.*, 2005, **44**, 2636–2639.
151 G. A. Olah, A. Goeppert and G. K. S. Prakash, Beyond Oil and Gas: The Methanol Economy, Wiley-VCH, 2006.
152 J. Graciani, K. Mudiyanselage, F. Xu, A. E. Baber, J. Evans, S. D. Senanayake, D. J. Stacchiola, P. Liu, J. Hrbek, J. F. Sanz and J. A. Rodriguez, *Science*, 2014, **345**, 546−550.
153 M. Nielsen, E. Alberico, W. Baumann, H.-J. Drexler, H. Junge, S. Gladiali and M. Beller, *Nature*, 2013, **495**, 85–89.
154 W. Leitner, E. Dinjus and F. Gassner, In Aqueous-Phase Organometallic Catalysis, Concepts and Applications, B. Cornils, W. A. Herrmann, Eds. Wiley-VCH: Weinheim, 1998; pp 486–498.
155 Y. Himeda, *Eur. J. Inorg. Chem.*, 2007, 3927–3941.
156 P. G. Jessop, Homogeneous hydrogenation of carbon dioxide. In Handbook of Homogeneous Hydrogenation, J. G. De Vries, Elsevier, C. J., Eds. Wiley-VCH: Weinheim, 2007; Vol. 1, pp 489–511.
157 C. Federsel, R. Jackstell and M. Beller, *Angew. Chem. Int. Ed.*, 2010, **49**, 6254–6257.
158 W. Wang, S. Wang, X. Ma and J. Gong, *Chem. Soc. Rev.*, 2011, **40**, 3703–3727.
159 W.-H. Wang and Y. Himeda, Recent advances in transition metal-catalysed homogeneous hydrogenation of carbon dioxide in aqueous media in Hydrogenation, Karamé (Ed.), ISBN: 978-953-51-0785-9, InTech, 2012.
160 Y. Izumi, *Coord. Chem. Rev.*, 2013, **257**, 171–186.
161 W.-H. Wang, Y. Himeda, J. T. Muckerman, G. F. Manbeck and E. Fujita, *Chem. Rev.*, 2015, doi:10.1021/acs.chemrev.5b00197
162 X. Yang, *ACS Catal.*, 2011, **1**, 849–854.
163 R. Tanaka, M. Yamashita and K. Nozaki, *J. Am. Chem. Soc.*, 2009, **131**, 14168–14169.
164 G. Zhao and F. Joó, *Cat. Comm.*, 2011, **14**, 74–76.
165 Y. Himeda, S. Miyazawa and T. Hirose, *ChemSusChem*, 2011, **4**, 487–493.

166 Y. Maenaka, T. Suenobu and S. Fukuzumi, *Energy Environ. Sci.*, 2012, **5**, 7360–7367.
167 S. Wesselbaum, U. Hintermair and W. Leitner, *Angew. Chem. Int. Ed.*, 2012, **51**, 8585–8588.
168 C. A. Huff and M. S. Sanford, *ACS Catal.*, 2013, **3**, 2412–2416.
169 K. Sordakis, M. Beller and G. Laurenczy, *ChemCatChem*, 2014, **6**, 96–99.
170 S. Moret, P. J. Dyson and G. Laurenczy, *Nature Comm.*, 2014, **5**, 4017.
171 J. L. Drake, C. M. Manna and J. A. Byers, *Organometallics*, 2013, **32**, 6891–6894.
172 S.-F. Hsu, S. Rommel, P. Eversfield, K. Muller, E. Klemm, W. R. Thiel and B. Plietker, *Angew. Chem. Int. Ed.*, 2014, **53**, 7074–7078.
173 R. Tanaka, M. Yamashita, L. W. Chung, K. Morokuma and K. Nozaki, *Organometallics*, 2011, **30**, 6742–6750.
174 G. A. Filonenko, R. V. Putten, E. N. Schulpen, E. J. M. Hensen and E. A. Pidko, *ChemCatChem*, 2014, **6**, 1526–1530.
175 G. O. Evans and C. J. Newell, *Inorg. Chim. Acta*, 1978, **31**, L387–L389;
176 C.-C. Tai, T. Chang, B. Roller and P. G. Jessop, *Inorg. Chem.*, 2003, **42**, 7340–7341.
177 S. Enthaler, K. Junge and M. Beller, *Angew. Chem. Int. Ed.* 2008, **47**, 3317–3321.
178 C. Ziebart, C. Federsel, P. Anbarasan, R. Jackstell, W. Baumann, A. Spannenberg and M. Beller, *J. Am. Chem. Soc.*, 2012, **134**, 20701–20704.
179 Y. Zhang, A. D. MacIntosh, J. L. Wong, E. A. Bielinski, P. G. Williard, B. Q. Mercado and N. Hazari, *Chem. Sci.*, 2015, **6**, 4291–4299
180 C. Federsel, C. Ziebart, R. Jackstell, W. Baumann and M. Beller, *Chem. Eur. J.*, 2012, **18**, 72–75.
181 M. S. Jeletic, M. T. Mock, A. M. Appel and J. C. Linehan, *J. Am. Chem. Soc.*, 2013, **135**, 11533–11536.
182 Y. M. Badiei, W.-H. Wang, J. F. Hull, D. J. Szalda, J. T. Muckerman, Y. Himeda and E. Fujita, *Inorg. Chem.*, 2013, **52**, 12576–12586.
183 H.-W. Suh, T. J. Schmeier, N. Hazari, R. A. Kemp and M. K. Takase, *Organometallics*, 2012, **31**, 8225–8236.
184 C. M. Zall, J. C. Linehan and A. M. Appel, *ACS Catal.*, 2015, **5**, 5301–5305.
185 B. Jezowska-Trzebiatowska and P. Sobota, *J. Organomet. Chem.*, 1974, **80**, C27–C28.
186 158 Y. Musashi and S. Sakaki, *J. Am. Chem. Soc.*, 2000, **122**, 3867–3877.
187 A. Urakawa, M. Iannuzzi, J. Hutter and A. Baiker, *Chem. Eur. J.*, 2007, **13**, 6828–6840.
188 C. Bo and A. Dedieu, *Inorg. Chem.*, 1989, **28**, 304–309.
189 P. G. Jessop, T. Ikariya and R. Noyori, *Chem. Rev.*, 1995, **95**, 259–272.
190 H. H. Karsch, *Chem. Ber.*, 1977, **110**, 2213–2221.
191 Y. Inoue, H. Izumida, Y. Sasaki and H. Hashimoto, *Chem. Lett.*, 1976, **5**, 863–864.
192 M. W. Farlow and H. Adkins, *J. Am. Chem. Soc.*, 1935, **57**, 2222–2223.
193 H. Wiener, J. Blum, H. Feilchenfeld, Y. Sasson and N. Zalmanov, *J. Catal.*, 1988, **110**, 184–190.
194 D. Preti, C. Resta, S. Squarcialupi and G. Fachinetti, *Angew. Chem., Int. Ed.*, 2011, **50**, 12551–12554.
195 C. Hao, S. Wang, M. Li, L. Kang and X. Ma, *Catal. Today*, 2011, **160**, 184–190.
196 D. Preti, S. Squarcialupi and G. Fachinetti, *ChemCatChem*, 2012, **4**, 469-471.
197 N. Liu, J. Lei, M. Y. Li and P. Wang, *Adv. Mat. Res.*, 2014, **283**, 881–883.
198 G. Peng, S. J. Sibener, G. C. Schatz and M. Mavrikakis, *Surf. Sci.*, 2012, **606**, 1050–1055.
199 Z. Xu, N. D. McNamara, G. T. Neumann, W. F. Schneider and J. C. Hicks, *ChemCatChem*, 2013, **5**, 1769–1771.
200 T. Maihom, S. Wannakao, B. Boekfa and J. Limtrakul, *J. Phys. Chem. C*, 2013, **117**, 17650–17658.
201 Y. Zhang, J. Fei, Y. Yu and X. Zheng, *Catal. Commun.*, 2004, **5**, 643–646.
202 Z. Zhang, Y. Xie, W. Li, S. Hu, J. Song, T. Zhiang and B. Han, *Angew. Chem., Int. Ed.*, 2008, **47**, 1127–1129.
203 Y. Amao, *ChemCatChem*, 2011, **3**, 458–474
204 K. R. Thampi, J. Kiwi and M. Grazel, *Nature*, 1987, **327**, 506–508.
205 T. Inoue, A. Fujishima, S. Konishi and K. Honda, *Nature*, 1979, **277**, 637–638.
206 B. Aurian-Blajeni, M. Halmann and J. Manassen, *Sol. Energy*, 1980, **25**, 165–170.
207 D. Mandler and I. Willner, *J. Chem. Soc., Perkin Trans.1*, 1988, **2**, 997–1003.
208 I. Willner and D. Mandler, *J. Am. Chem. Soc.*, 1989, **111**, 1330–1336.
209 I. Willner, N. Lapidot, A. Riklin, R. Kasher, E. Zahavy and E. Katz, *J. Am. Chem. Soc.*, 1994, **116**, 1428–1441.
210 I. Willner, I. Willner and N. Lapidot, *J. Am. Chem. Soc.*, 1990, **112**, 6438–6439.
211 K. Schuchmann and V. Müller, *Science*, 2013, **342**, 1382–1385.
212 A. Alissandratos, H.-K. Kim and C. J. Easton, *Bioresource Techno.*, 2014, **164**, 7–11.
213 M. Kodaka and Y. Kubota, *J. Chem. Soc., Perkin Trans.1*, 1999, **2**, 891–894.
214 R. Miyatani and Y. Amao, *Biotechnol. Lett.*, 2002, **24**, 1931–1934.
215 R. Miyatani and Y. Amao, *J. Mol. Catal. B*, 2004, **27**, 121–125.
216 R. Miyatani and Y. Amao, *J. Jpn. Pet. Inst.*, 2004, **47**, 27–31.
217 I. Tsujisho, M. Toyoda and Y. Amao, *Catal. Commun.*, 2006, **7**, 173–176.
218 S. Sato, T. Morikawa, S. Saeki, T. Kajino and T. Motohiro, *Angew. Chem., Int. Ed.*, 2010, **49**, 5101–5105.
219 T. Arai, S. Tajima, S. Sato, K. Uemura, T. Morikawa and T. Kajino, *Chem. Commun.*, 2011, **47**, 12664–12666.
220 S. Sato, T. Arai, T. Morikawa, K. Uemura, T. M. Suzuki, H. Tanaka and T. Kajino, *J. Am. Chem. Soc.*, 2011, **133**, 15240–15243.
221 T. Arai, S. Sato, K. Uemura, T. Morikawa, T. Kajino and T. Motohiro, *Chem. Commun.*, 2010, **46**, 6944–6946.
222 T. M. Suzuki, H. Tanaka, T. Morikawa, M. Iwaki, S. Sato, S. Saeki, M. Inoue, T. Kajino and T. Motohiro, *Chem. Commun.*, 2011, **47**, 8673–8675.
223 A. Nakada, K. Koike, T. Nakashima, T. Morimoto and O. Ishitani, *Inorg. Chem.*, 2015, **54**, 1800–1807.
224 E. E. Benson, C. P. Kubiak, A. J. Sathrum and J. M. Smieja, *Chem. Soc. Rev.*, 2009, **38**, 89–99.

225 H. Arakawa, M. Aresta, J. Armor, M. Barteau, E. Beckman, A. Bell, J. Bercaw, C. Creutz, D. A. Dixon, D. Dixon, K. Domen, D. DuBois, J. Eckert, E. Fujita, D. Gibson, W. Goddard, D. Goodman, J. Keller, G. Kubas, H. Kung, J. Lyons, L. Manzer, T. Marks, K. Morokuma, K. Nicholas, R. Periana, L. Que, J. Rostrup-Nielson, W. Sachtler, L. Schmidt, A. Sen, G. Somorjai, P. Stair, B. Stults and W. Tumas, *Chem. Rev.*, 2001, **101**, 953–996.
226 W. Leitner, *Angew. Chem. Int. Ed.*, 1995, **34**, 2207–2221.
227 F. A. de Bruijn, D. C. Papageorgopoulos, E. F. Sitters and G. J. M. Janssen, *J. Power Sources*, 2002, **110**, 117–124.
228 R. K. Ahluwalia and X. Wang, *J. Power Sources*, 2008, **180**, 122–131.
229 A. E. Russell, S. C. Ball, S. Maniguet and D. Thompsett, *J. Power Sources*, 2007, **171**, 72–78.
230 S. Giddey, F. Ciacchi and S. Badwal, *Ionics*, 2005, **11**, 1.
231 T. Tingelöf, L. Hedström, N. Holmström, P. Alvfors and G. Lindbergh, *Int. J. Hydrogen Energy*, 2008, **33**, 2064–2072.
232 J. Larminie and A. Dicks, Fuel cell systems explained, Wiley, Chichester, 2003.
233 P. Bernardo, E. Drioli and G. Golemme, *Ind. Eng. Chem. Res.*, 2009, **48**, 4638–4663.
234 R. Williams, R. S. Crandall and A. Bloom, *Appl. Phys. Lett.*, 1978, **33**, 381–383.
235 M. Halmann, M. Ulman and B. Aurian-Blajeni, *Sol. Energy*, 1983, **31**, 429–431.
236 H. Wiener, Y. Sasson and J. Blum, *J. Mol. Catal.*, 1986, **35**, 277–284.
237 B. Zaidman, H. Wiener and Y. Sasson, *Int. J. Hydrogen Energy*, 1986, **11**, 341–347.
238 H. Wiener, B. Zaidman and Y. Sasson, *Sol. Energy*, 1989, **43**, 291–296.
239 S. Enthaler, *ChemSusChem*, 2008, **1**, 801–804.
240 F. Joo, *ChemCatChem*, 2014, **6**, 3306–3308.
241 S. Fukuzumi, *Eur. J. Inorg. Chem.*, 2008, 1351–1362.
242 Q. L. Zhu and Q. Xu, *Energy Environ. Sci.*, 2015, **8**, 478–512.
243 P. Sponholz, D. Mellmann, H. Junge and M. Beller, *ChemSusChem*, 2013, **6**, 1172–1176.
244 A. Boddien, C. Federsel, P. Sponholz, D. Mellmann, R. Jackstell, H. Junge, G. Laurenczy and M. Beller, *Energy Environ. Sci.*, 2012, **5**, 8907–8911.
245 S.-F. Hsu, S. Rommel, P. Eversfield, K. Muller, E. Klemm, W. R. Thiel and B. Plietker, *Angew. Chem. Int. Ed.*, 2014, **53**, 7074–7078.
246 A. Boddien, F. Gärtner, C. Federsel, P. Sponholz, D. Mellmann, R. Jackstell, H. Junge and M. Beller, *Angew. Chem. Int. Ed.*, 2011, **50**, 6411–6414.
247 Q.-Y. Bi, J.-D. Lin, Y.-M. Liu, X.-L. Du, J.-Q. Wang, H.-Y. He and Y. Cao, *Angew. Chem. Int. Ed.*, 2014, **53**, 13583–13587.
248 J. Su, L. Yang, M. Lu and H. Lin, *ChemSusChem*, 2015, **8**, 813–816.

Graphical Abstract

Formic acid, the simplest carboxylic acid, could serve as one of the better fuel for portable devices, vehicles and other energy related applications in future.